Diel cycles of *Prochlorococcus* spp. across the north Pacific subtropical gyre

BY

Star Dressler

A thesis submitted in partial fulfillment of the

requirements for the degree of

MASTER OF SCIENCE

IN

BIOLOGY

UNIVERSITY OF GUAM

July 19, 2024

Title: Diel cycles of *Prochlorococcus* spp. across the north Pacific subtropical gyre

Approved: _____
Atsushi Fujimura, Chair, Thesis Committee

Abundance and growth rate of photosynthesizing microorganisms are drivers of primary productivity in marine environments. These primary producers form the foundation of the trophic food web and are influenced by abiotic factors including sea surface temperature and nutrient availability. This research effort works toward the goal of standardizing data collection of phytoplankton ecosystem functioning across ocean transects. Marine autotrophic plankton exhibit photosynthesis-driven diel patterns of cell size that may be modeled to growth rates, and concurrent environmental variables may be quantitatively investigated as drivers on shifts in growth rates. This data, collected in the summer of 2022 on a research vessel transect across the 30° N latitude line through the north Pacific subtropical gyre, used 53 days of continuous side scatter data of individual *Prochlorococcus* cells, converted this data into cellular carbon content, and fit this data into a sine function to model growth rates. Within the gyre, surface waters are oligotrophic and exhibit a small range of sea surface temperatures. Statistical results and patterns across datasets point toward nutrient availability as the main driver on shifts in *Prochlorococcus* growth rates. Moving west to east, the influx of nutrients toward surface waters weakened, and less nutrient availability led to smaller cell biomass and weakened growth rates.

ACKNOWLEDGEMENTS

I would like to extend my gratitude to my Marine Lab cohort that assisted in the stabilization of my mental health during this process: Sarai Vega, Adam Perez, Andrew O'Neill, Therese Miller, and Grace Jackson. Thank you to my advisor, Atsushi Fujimura, for staying with me through the ride of two separate thesis proposals. Thank you to Nicole Poulton for first inviting me to the P02 cruise, and thanks to the other Bio-GO-SHIP members for making this project possible: Adam Martiny, Sophie Clayton, Jason Graff, and Luke Thompson. Thank you to my parents and extended family for supporting me through my unconventional journey to this point in time.

This work was supported by the National Science Foundation under Grant No. OIA-1946352

Contents

List of Tables

List of Figures

1. Introduction

Abundance and growth rate of photosynthesizing microorganisms are drivers of primary productivity in marine environments. The rate of photoassimilation of organic carbon by autotrophs is referred to as gross primary production, and net primary production (NPP) is the rate of dark respiration, or the oxidation of organic carbon back to carbon dioxide, subtracted from the gross primary production (Bender et al., 1987). Terrestrial and oceanic systems contribute equally to global NPP, making marine phytoplankton responsible for about half of the planet's photosynthetic processes and biosynthesis of organic compounds (Field et al., 1998). Primary producers form the foundation of the trophic food web, thus regulating trophic level dynamics (Fenchel, 1988; Krumhardt et al., 2022), and the cycling of carbon regulates the rate of carbon sinks (Eppley & Peterson, 1979; Petrou et al., 2016).

These biological processes are influenced by abiotic factors including ocean temperature and nutrient availability. Biogeochemical shifts resulting from changing climate, as predicted by some Earth system models, may include intensified vertical stratification, driven by the warming of surface waters, that limits the diapycnal influx of nutrients to surface waters and triggers a decline in NPP (Bopp et al., 2013; Fu et al., 2016). Alongside these predictions, it is important to consider the potential resilience of some primary producers (Martiny et al., 2022).

There is a paradox within the predicted fates of marine phytoplankton, where consequences of ocean warming may limit primary productivity, but warmer water temperatures may also stimulate their growth rate (Behrenfeld, 2011; Taucher & Oschlies, 2011). Inorganic nutrient availability also impacts growth rates of phytoplankton, though the picocyanobacterium *Prochlorococcus* is noted to dominate in oligotrophic conditions and nutrient amendment experiments do not always impact growth rates (K. Liu et al., 2021; Worden & Binder, 2003). To

better understand the impact of multiple drivers on shifts in planktonic communities over time, it is key to standardize the methodology of in situ data collection on plankton community structure, estimated individual cell size, and abundance at appropriate temporal and spatial scales. These parameters may be used to estimate the in situ growth rates of phytoplankton species and functional groups, and concurrent abiotic variables, including water temperature and inorganic nutrient availability, may be quantitatively investigated as potential drivers on these growth rates.

Marine autotrophic plankton generally exhibit diel patterns of a photosynthesis-driven increase of individual cell volume during daylight hours, and a nighttime decrease of individual cell volume from respiration and cell division (DuRand, 1995). The amplitude of this daily cell volume oscillation is proportional to cell size. Changes in cell size distributions over a time series can be modeled to provide an estimate of daily division rate. The frequency of dividing cells corresponds to net growth rate (Hunter-Cevera et al., 2014). Understanding in situ growth rates of marine phytoplankton is a vital component of monitoring shifts in global NPP. Ship-based data collection efforts grant the opportunity to gather information on diel patterns of cell volume which can be incorporated into growth rate modeling, along with concurrent in situ measurements of abiotic variables such as inorganic nutrient composition and water temperature. This research uses 53 days of data collected during the P02 transect in May-July 2022 by the Biological Global Ocean Ship-Based Hydrographic Investigations Program (Bio-GO-SHIP). Continuous flow cytometry (FCM) data of pico-nanoplankton in surface waters provides information about diel changes in cell volume and environmental variables across the 30° north latitude line from Japan to California in the Pacific Ocean.

1.1 Traditional Dilution Experiments

Understanding biological and environmental factors that regulate picophytoplankton populations has been traditionally investigated via dilution assays. This technique discerns true picophytoplankton growth and grazing mortality from net phytoplankton growth, with the assumption that increasingly more dilute samples experience less impact from grazing (Gallegos, 1989; Landry & Hassett, 1982). In this methodology, the series of dilutions are incubated for 24 hours. Picophytoplankton are identified and enumerated by FCM, and net growth rates are determined based on cell counts at time 0 and 24 hours. A basic assumption in this methodology is that grazing impact is a linear function of the dilution amount. More conservative estimates of growth and mortality rates may be derived from non-linear results (Worden & Binder, 2003).

There are many methodical modifications that a researcher may make to the dilution assay approach for estimating phytoplankton mortality. This generates variation in the assessments of growth rates, complicating the ability to make intercomparisons between publications. Researchers have called for greater standardization in methodology and the presentation of results (Staniewski & Short, 2018). Using diel shifts in cell size to model growth rates has recently been implemented, with Hunter-Cevera, et al. 2014 comparing modeling results to dilution series experiments as a form of model evaluation. Across a range of division and loss rates, the dilution experiments agreed well with the modeled division rates. The modeling approach uses continuous FCM data and provides a dramatic increase of resolution with more daily division rates obtained over a period of time. This increased resolution applied over a timeseries allows for the quantitative investigation of potential environmental drivers on observed shifts in growth rates (Hunter-Cevera et al., 2014).

1.2 Bio-GO-SHIP

The Global Ocean Ship-Based Hydrographic Investigations Program (GO-SHIP, https://www.go-ship.org) documents global ocean change through systematic decadal observations of physical and biogeochemical parameters throughout the full water column. This research effort is a network of 55 globally coordinated hydrographic transects (Sloyan et al., 2019). GO-SHIP is the current framework that follows previous global repeat survey iterations, including Geochemical Ocean Sections Study (GEOSECS; Moore, 1984), the World Ocean Circulation Experiment (WOCE; Woods, 1985), and the Joint Global Ocean Flux Study (JGOFS; Anderson et al., 2001). The array of measurements performed during GO-SHIP transects are considered physical and chemical Essential Ocean Variables (EOVs), which are defined as measured variables that assist policymaking in the understanding, management, adaption, and mitigation of global ocean change (Miloslavich et al., 2018). EOVs measured by GO-SHIP have evolved our understanding of shifts in ocean physical biogeochemistry, including deep-ocean warming, deep-ocean salinity and freshening, circulation, vertical diffusivities, transport, mixing, inorganic carbon and dissolved organic carbon fluxes, anthropogenic transient-tracers, radiocarbon, ventilation, etc. (Talley et al., 2016).

Global repeat hydrographic surveys have historically under-sampled biological ocean processes as compared to the efforts to measure chemical and physical parameters. Biological processes, including organism abundance, diversity, and ecosystem functioning are challenging to quantify in situ at appropriate spatial and temporal scales. Satellite-derived measurements of ocean color in surface waters provide valuable insight at high-temporal resolution to global planktonic chlorophyll/biomass (Noh et al., 2022), net primary production (Behrenfeld et al., 2005), and carbon transport (Siegel et al., 2016). Ship-based in situ data collection provides the opportunity to continuously in situ sample at finer spatial scales across a transect. Several

methodologies to understand biological processes are currently being integrated into the existing GO-SHIP framework through Biological GO-SHIP (Bio-GO-SHIP, https://biogoship.org/). Bio-GO-SHIP utilizes a suite of modern technologies to develop standard and relevant biological observation protocols that have the potential to be broadly applied to other research efforts beyond GO-SHIP.

The biological and ecological EOVs of Bio-GO-SHIP includes microbial, phytoplankton, zooplankton, and fish biomass and diversity. Quantifying these EOVs has the potential to fill in knowledge-gaps surrounding plankton biodiversity, interactions between planktonic community structure and ecosystem functioning on chemical inventories, and the physical connectivity of biological communities of interest. More broadly, there is potential to merge biological observations with concurrent physical and chemical parameters across many temporal and spatial scales. The methods currently implemented at sea by Bio-GO-SHIP includes ‘omics (eDNA and RNA), optical, imaging, and particulate measurements of phytoplankton (Clayton et al., 2022).

1.3 Flow Cytometry and Modeling Phytoplankton Growth Rates

Deriving in situ growth rates at appropriate time scales within physically dynamic environments has historically challenged researchers, and open ocean biological sampling methods have often had poor spatial and temporal resolution. Using a shipboard FCM to continuously track diel shifts in cell size across a transect may be an insightful and accessible method for tracking changes in phytoplankton EOVs into the future. Diel shifts in cell sizes and phytoplankton abundance data may be modeled as phytoplankton growth rates; however, this relationship was first understood through the measurements of the frequency of dividing cells.

The relationship between the frequency of dividing cells and growth rate in aquatic systems has been investigated and modeled for decades (Hagström et al., 1979). Prior to this research, the ecosystem functioning of free-living microbes in pelagic systems was not understood. Through in situ sampling efforts compared with controlled in vitro conditions, Hagström et al., 1979 began to formally establish the relationship between frequency of dividing cells and growth rate. Further publications expanded on this relationship, focusing on cyanobacterial growth rates (Campbell & Carpenter, 1986) and ecosystem functioning (Hagström et al., 1988).

These previously noted publications use epifluoresence counts of individual cells to estimate the frequency of dividing cells. The development of automated FCMs (Dubelaar et al., 1999; Olson et al., 1990) allowed for the continuous documentation of individual cell size and taxonomic grouping of planktonic organisms, thus expanding the range of scales that these organisms can be studied. FCMs optically stimulate individual cells, gathering information on the directionality of the scattered photons (forward scatter, or FSC, and side scatter, or SSC), as well as the fluorescence signature, of each cell. These parameters assist in the identification of some phytoplankton taxonomic groups (Tarran et al., 2006). Scattering phase function is dependent upon the cell's size and refractive index (Bohren & Huffman, 1983). Differential FSC and SSC measurements of *Prochlorococcus* across the Atlantic reveals regimes of enhanced scattering that follow the thermocline depth, and distinctions between the northern and southern gyres (Smyth et al., 2023).

Building off observations of diel variations of bulk water optical beam attenuation in marine systems, DuRand, 1995 examined how the optical properties of phytoplankton are impacted by cell growth and division. Laboratory-based diel experiments compared to in situ

data from the equatorial Pacific revealed that FCM measured phytoplankton assemblages accounted for nearly all the diel variation in beam attenuation signal. Nanoplankton (identified as 2-20 μm, mostly 2-3 μm) were noted as the greatest contributor to total attenuation by phytoplankton, while ultraphytoplankton (1-2 μm diameter) exhibited greater contribution to diel variation of this signal. Results of this work demonstrated how an increase of cell volume during daylight can be translated to a minimum estimate of daily division rate, while assuming that population cell growth and division are separated in time (DuRand, 1995).

Using a submersible FCM called the FlowCytobot, Sosik et al., 2003 generated a 2-month time series of diel shifts in cell scattering of pico-nanoplankton from Atlantic offshore surface waters. With shifts in cell scattering interpreted as shifts in individual cell size, the continuous size distribution data was incorporated into a size-structured matrix population model (Caswell, 2001) that can estimate daily specific growth rates of *Synechococcus*. This model approach was novel in its ability to incorporate the full size distribution of the population, as well as accounting for simultaneous cell growth and division. The size distribution method can determine cell-specific growth rates that are independent of shifts in cell concentration, which allows for the separation of the effects of natural mortality, grazing, viral infection, and mixing of populations via mixing of water masses (Sosik et al., 2003).

The work of Hunter-Cevera et al., 2014 expanded the timescale of which *Synechococcus* growth rates were estimated via matrix population modeling, as well as developing correlations of shifts in growth rates with concurrent in situ biogeochemical processes. Continuous annual FCM data from Atlantic coastal surface waters, partitioned into hourly samples of cell size distributions, showed distinct seasonal patterns in division rates that result from small environmental shifts. These shifts occur over a timespan of weeks to months and favors either

net cell growth or loss. Temperature likely regulates division rates during the first half of the year, while light and temperature limits division rates in the winter. High division rates were found to persist over periods of time with little shift in cell abundance (Hunter-Cevera et al., 2014).

With cell size distribution datasets that span several years, this methodology has potential to examine environmental drivers of shifts in phytoplankton bloom timing. Hunter-Cevera et al., 2016 reported that over a 13-year hourly time series, the timing of the Atlantic coastal bloom of *Synechococcus* varied by four weeks. The seasonal onset of warming sea surface temperature was the main mechanism affecting bloom timing, with temperature-induced impacts on both cell division rates and earlier blooms driven by warmer surface waters in the spring (Hunter-Cevera et al., 2016). Both reports show a correlation between *Synechococcus* loss rates and division rates, which suggests a balance between growth and loss that persists over time despite environmental and phenological shifts (Hunter-Cevera et al., 2014, 2016). Additionally, Hunter-Cevera et al., 2016 revealed a significant positive correlation between net growth rates and division rates during the spring bloom.

When considering the bulk properties of phytoplankton via satellite data, which generally aggregates the phytoplankton community as a whole, the correlation between abiotic variables and division rates has been argued as an invalid driver of phytoplankton blooms, and that bloom dynamics are instead driven by climate forcings and food-web shifts (Behrenfeld & Boss, 2014). Conversely, Hunter-Cevera et al., 2016 utilized finer spatial, temporal, and taxonomic resolution to reveal a strong correlation between temperature, division rates, and phenological shifts within *Synechococcus*; however, the resilience of these ecological couplings is uncertain as warming trends continue (Hunter-Cevera et al., 2016). Continued observances through Hunter-Cevera's

work enforced that drivers shift seasonally, with temperature limiting cell division in winter and spring, and light limiting cell division in the fall. Seasonality within *Synechococcus* loss processes observed over this cumulative 16-year time series show the importance of examining the taxonomy, abundance, and ecological activity of predators that target this cyanobacterium (Hunter-Cevera et al., 2020).

Matrix population models have recently been experimentally improved to include additional biological process that describe population dynamics over the diel cycle, including cell division, carbon fixation, and carbon loss associated with laboratory cultures of *Prochlorococcus*. Using a Bayesian framework for the models permits the incorporation of prior information in order to regulate parameter inference, and to avoid biologically implausible parameter values. Though improvements are necessary, there is flexibility within this modeling framework that may be able to incorporate more complex datasets, including shipboard FCM data (Mattern et al., 2022). Currently, there are few publications that give precedence to modeling phytoplankton dynamics from a transect transversed by a moving ship. Larkin et al., 2020, 2023; Ustick et al., 2021, 2023 all utilized metagenomic data from Bio-GO-SHIP to compare phytoplankton diversity to an array of environmental variables. Ribalet et al., 2015 used continuous FCM data from two Pacific transects to incorporate *Prochlorococcus* cell size distributions into a matrix population model, as well as estimates of daily carbon production and ecotype composition, to examine the diel synchrony of cell growth and mortality across the subtropical Pacific gyre.

1.4 Abiotic Variables

1.4.1 Water Temperature

Water temperature regulates the rate of biochemical reactions in microbes, which includes the rate of *Prochlorococcus* cell division. Generally, rates of biochemical reactions increase with warmer temperature until an optimal temperature is reached, and at further increased temperatures these rates will decrease rapidly (Ratkowsky et al., 1983). For photosynthesizing microorganisms, the carbon to chlorophyll ratio increases linearly with increasing light at constant temperature, and decreases exponentially with elevated and increasing temperature at constant light (Geider, 1987).

The probability of detecting *Prochlorococcus* in water samples increases with increased water temperatures. Between 8 °C and 13 °C, the probability increases from 20% to 80%, and above 13 °C, the probability is between 80 % to ~100%. Between 8 °C and 13 °C, *Prochlorococcus* cell abundances are generally 10^4 cells mL^{-1}, and above 13 °C the abundances increase to 10^5 cells mL^{-1} (Flombaum et al., 2013). Temperature growth optima in cultured isolates of *Prochlorococcus* is recognized to correlate well with ecotype distribution in the Atlantic ocean (Zinser et al., 2007). Ribalet et al., 2015 used a size-structured matrix population model on continuous size distribution data of *Prochlorococcus* across two open ocean transects in the eastern Pacific. Cooler waters (16 °-19 °C) were associated with lower cell division rates, while warmer subtropical gyre waters were associated with higher cell division rates, and each of these regions were dominated by a different ecotype of high-light-adapted *Prochlorococcus*. The highest division rate (0.9 d^{-1}) occurred at 25 °C in low-latitude waters and is similar to the highest division rate reported for cultures of the same *Prochlorococcus* ecotype grown in nutrient-deplete conditions (Ribalet et al., 2015).

Reports show a seasonal link between water temperature, rates of cyanobacterial cell division, and timing of blooms (Hunter-Cevera et al., 2020), as well as between temperature regimes and functional gene content (Ustick et al., 2023). Some *Prochlorococcus* ecotypes are associated with temperature regimes, including high-light, low temperature clade (eHL-I), and high-light, high-temperature clade (eHL-II). A crossover point of the domination of one of these ecotypes over the other has been found to occur at ~21°C in the Eastern Indian Ocean (Larkin et al., 2020), which matches the transition temperature noted for these ecotypes in the North Pacific Ocean, though these dynamics are likely subject to seasonality (Larkin et al., 2016). Generally, the dynamics between *Prochlorococcus* and temperature regimes demonstrates the uncertainties of how changing climate may impact the distribution and ecosystem functioning of populations globally.

1.4.2 Nutrient Composition and Supply Flux

Prochlorococcus dominates in oligotrophic conditions and is noted to be typically a hundred times more abundant than *Synechococcus*, with the exception of areas that have constant or transient influx of nutrient enrichment from coastal input or upwelling (Partensky, Blanchot, et al., 1999). Growth rates of *Synechococcus* from a 16-year dataset of hourly observations show little sensitivity to the inorganic nutrient environment; seasonal increases in growth rates are more so driven by temperature. Nutrient data throughout this research is sparse, but indicates that division rates have no systematic limitation via nutrients. Nutrients may play a role in sudden variations in division rates, such as interspersed low division rates, which may persist for multiple days in a row, in summer when division rates are generally high (Hunter-Cevera et al., 2020).

Regarding *Prochlorococcus*, ambient inorganic nutrient concentrations have been found to influence ecotype composition. Additionally, there are clades that exhibit differences in nutrient assimilation. *Prochlorococcus* was long assumed to not be able to assimilate nitrate, until genomics identified nitrite and nitrate assimilation genes from various global ecotypes (Berube et al., 2015; Martiny et al., 2009). This cyanobacterium has also been associated with phosphorous assimilation genes (Martiny et al., 2009), and phosphate levels have been found to correlate with *Prochlorococcus* haplotype (Larkin et al., 2020). Generally, *Prochlorococcus* adapts to low-nutrient conditions via gene loss and gains, resulting in a correlation of genome content and locally available nutrients (Partensky & Garczarek, 2010). High nutrient, low chlorophyll regions of the ocean, which are often replete with macronutrient levels but low in iron availability, are associated with unique *Prochlorococcus* clades (Rusch et al., 2010; Ustick et al., 2021). The modern understanding of *Prochlorococcus* genomics can be interpreted to represent global-scale patterns of ocean nutrient limitation. Laboratory bottle experiments, *Prochlorococcus* gene stress, and Earth system model predictions agree to show global regional transitions in nutrient stress type, severity, and co-stress of multiple nutrient types (Ustick et al., 2021).

The stoichiometry of particulate organic matter (ratio of carbon to nitrogen to phosphorus; C:N:P), or the plankton elemental requirements, within marine systems is a method utilized to examine dynamics in planktonic community structure and ecosystem functioning (Moreno & Martiny, 2018). Higher latitudes exhibit temperature as a main driver of shifts in stoichiometry, while lower latitudes transition to a stronger nutrient dependency, likely due to decreased nutrient supply rates in lower latitudes (Tanioka et al., 2022). Nutrient limitation can suppress the temperature dependence of phytoplankton metabolic rates (Marañón et al., 2018;

Thomas et al., 2017). In *Prochlorococcus,* temperature positively affects the carbon and nitrogen cell quota, whereas phosphorous cell quota shows no significant trend. There are complex correlations between individual elemental ratios and *Prochlorococcus* strain identity, growth rate, and temperature that are indicative of lineage-unique cellular elemental effects that may result from rising water temperatures (Martiny et al., 2016).

1.4.2.1 Nutricline

Due to inorganic nutrient levels being generally low/at detectable levels in surface waters throughout much of the low latitude open ocean, nutrient supply may be examined as a potential driver on shifts in growth rates. This research utilizes nutricline depth as a proxy for the diapycnal influx of inorganic nutrients to the mixed layer (Cermeño et al., 2008). The depth of the nutricline is dependent on the degree of stratification throughout the water column, as well as the strength of momentum transfer due to wind stress (Denman & Gargett, 1983). As physical mixing increases, the nutricline is penetrated by the upper mixed layer, providing nutrients to the euphotic zone. Contrarily, increased thermal stratification will create a density barrier between the upper mixed layer and the nutricline; the nutricline will progressively deepen, generally parallel to the depth of the euphotic zone. In the subtropical open ocean, the flux of nutrients is largely limited to diffusive properties. Generally, the depth of the nutricline is in an inverse relationship with primary productivity of phytoplankton, which suggests that the rate of nutrient supply to the surface waters impacts photosynthetic performance (Behrenfeld et al., 2005; Cermeño et al., 2008).

A shallower nutricline depth is indicative of increased macronutrient availability toward the surface, as comparative to an increased nutricline depth (Richardson & Bendtsen, 2019). The

nutricline depth, as it relates to nitrate concentrations, has been found to correlate strongly with *Prochlorococcus* ecotype. Larkin et al., 2020 states that increased macronutrient availability may explain areas with shoaled nutricline depths and concurrent increased relative abundance of specific *Prochlorococcus* ecotypes, while areas with deeper nutriclines may explain the increased relative abundance of different ecotypes (Larkin et al., 2020). Deep thermoclines and nutriclines have also been linked to lower *Prochlorococcus* cell stocks in the Northern Atlantic Gyre (Lange et al., 2018).

Considering cell physiology, smaller cells have an increase of the cell-surface-to-volume ratio. This increase of cell surface with smaller cell size optimizes the absorption of incident photons (Dufresne et al., 2005). In the most nutrient-poor surface waters of the world, high light adapted ecotypes of *Prochlorococcus* dominate. Additionally, the genomes of these ecotypes are streamlined as compared to other ecotypes. This minimalism of genomic content allows for relative ease of cell propagation in nutrient deplete environments (Partensky & Garczarek, 2010).

1.4.3 Light and the Mixed Layer

The marine mixed layer represents surface waters with minimal stratification. Wind and tidal driven turbulence maintain the largely homogenous physical properties throughout this layer, which rests on top of the pycnocline. Passing weather fronts generate increased tidal and inertial forces that dissipate through the water column via subsurface waves, which can shear the mixed layer-pycnocline interface (Mann & Lazier, 2006; Stewart, 2008). *Prochlorococcus* eco-genotypes may occupy niches based along a depth gradient, though it is important to consider how water masses may be mixing at the time of sampling (Malmstrom et al., 2010; Zinser et al., 2007).

From the surface waters to the pycnocline, there is a descending gradient of irradiance. Light is a key ecological determinant of *Prochlorococcus* ecotype niches (Partensky et al., 1999). High light and low light adapted ecotypes have differing minimum, maximum, and optimal light intensities for facilitating growth (L. R. Moore & Chisholm, 1999). A significant number of genes are not commonly shared between these ecotypes, emphasizing a dynamic genome that is responding to selection pressures. Additionally, *Prochlorococcus* can utilize different forms of inorganic nitrogen that is more abundant at the given light level (Rocap et al., 2003).

For phytoplankton, the diel cycle is highly synchronized with the cell cycle. Cell growth occurs during daylight hours, and each functional group of picophytoplankton varies in the timing of their diel cell cycles (Vaulot & Marie, 1999). Diel oscillations occur in cell abundance, but are tightly coupled with mortality, which results in no net increase of population size over the diel cycle. Regardless of the ecotype composition of *Prochlorococcus*, cell division is recognized to peak near dusk and correspond with a decrease of mean cell size (Ribalet et al., 2015). *Prochlorococcus* haplotypes additionally exhibit unique diel oscillations amongst themselves (Larkin et al., 2020). The distinct synchronized diel patterns of cell size, though they are dynamic across many variables, may be incorporated into the modeling of growth rates.

Photosynthetically active radiation (PAR) is a commonly collected variable to understand the impacts of light on a system, and PAR intensity strongly correlates with *Prochlorococcus* abundances. At sea surface temperature of 20 °C, abundances are relatively low at very small PAR values and increase by 1-2 orders of magnitude with increasing PAR. At extremely high PAR values, there is a 31% decrease of cell abundances relative to peak abundances. However, low PAR values can still be associated with substantial cell abundances. The control of PAR on

cyanobacterial populations is complex and other environmental factors must be considered, such as nutrient availability at the given location (Flombaum et al., 2013).

1.5 Study Organism and Area

1.5.1 Study Organism

Prochlorococcus is a marine cyanobacterium found globally with noted phylogenetic diversity. This picophytoplankter (sized ~0.2-2 μm) was first reported in 1988, discovered via highly sensitive FCM and immediately recognized for its abundance throughout the euphotic zone. *Prochlorococcus* is recognized as a distinct population by its unique combination of pigments, particularly the lack of orange fluorescence that is generated by phycoerythrin, which is exhibited by the cyanobacterium *Synechococcus* (Chisholm et al., 1988). Following its reported discovery, *Prochlorococcus* was found to be the most abundant marine phytoplankton in tropical and subtropical oligotrophic waters between latitudes 40° N and 40° S (Partensky et al., 1999).

Different phylogenetic clades, or ecotypes, of *Prochlorococcus* exhibit unique adaptations for light, temperature, and iron availability (Bouman et al., 2006; L. R. Moore et al., 1998; Rusch et al., 2010). These distinct populations have more recently been researched as natural biosensors that can indicate subtle biogeochemical shifts (Larkin et al., 2020). *Prochlorococcus*' abundance, global distribution of populations, and access to isolates make it an ideal model system for examining biogeochemical ocean processes and microorganism diversity.

Rigorous statistical modeling of global *Prochlorococcus* abundance, based on >35,000 discrete samples, found highest abundances in the Indian and Western Pacific oceans, and more generally in warm, oligotrophic waters. Maximum abundances in these areas were between 2.1-

2.5 x 10^5 cells mL^{-1}, while in lower latitude waters (30°N to 30°S) mean abundances were 2.8 x 10^3 cells mL^{-1}. Cell abundances were low beyond 40°N and 40°S. Statistical model projections of the sea surface abundance of *Prochlorococcus* for the end of the 20th and 21st centuries, utilizing climate model projections of increased sea surface temperatures, predicts an 28.7% increase of global *Prochlorococcus* abundances. These projections are found to be the most significant in the Pacific Ocean (Flombaum et al., 2013).

1.5.2 Study Area

Within the north Pacific subtropical gyre (NPSG), nutrient conditions are largely oligotrophic, though environmental anomalies and eddies can trigger rare phytoplankton blooms within what is typically an oceanic desert (Chow et al., 2019). The planktonic community structure in similar regions is numerically dominated by *Prochlorococcus*, and despite the population doubling time of approximately one day, cell abundances stay relatively constant at nearly half a billion cells per liter (Partensky et al., 1999). Chlorophyll levels are seasonally lowest during summer in the NPSG due to constraints on the mixing of nutrients into the photic zone (Signorini & McClain, 2012).

The western equatorial Pacific is relatively more oligotrophic and can exhibit higher temperatures as compared to the eastern equatorial region. Measurable nutrients can be found in the eastern equatorial Pacific surface waters and increased primary productivity throughout the mixed layer. Concurrently, abundances of *Prochlorococcus* can be nearly double in the western region as compared to abundances in the east, contributing to 39% of the gross primary production in the west and 9% in the east. The NPSG at Station ALOHA (22° 45’ N, 150° W), is nutrient deplete throughout the mixed layer and exhibits high abundances of *Prochlorococcus*.

At Station ALOHA, *Prochlorococcus* has been found to contribute up to 82% of the gross primary production (Liu et al., 1997).

The western edge of the NPSG is at the boundary of the western Pacific warm pool, which transports heat to higher latitudes via the Kuroshio Current (Hu et al., 2015). Over the past decades, this oligotrophic region is understood to be increasing in sea surface temperature warming rate related to intensification of the Kuroshio Current (Wu et al., 2012). Phytoplankton communities in this region are dominated *Prochlorococcus* and *Synechococcus* (Endo & Suzuki, 2019), and these community structures may be adapted to local conditions and therefore, be vulnerable to environmental change (Thomas et al., 2017). The western edge of the gyre, with warm and oligotrophic conditions, is noted to have among the highest abundances of *Prochlorococcus* globally (Flombaum et al., 2013). The eastern edge of the NPSG is within the California Current system, bringing northern waters southwestward. Upwelling in the California Current system brings nutrients to surface, and may limit *Prochlorococcus* dominance, but seasonal patterns that suppress coastal upwelling may ephemerally increase *Prochlorococcus* abundances in these areas. The largest marine heat wave on record occurred in the winter of 2013-14 in the Gulf of Alaska. This event was associated with climate forcing of the North Pacific Oscillation and its effects lasted through early 2016. Heat wave events and additional climate change patterns will likely have a significant impact on phytoplankton abundances and community structure (Landry et al., 2024).

Phytoplankton in the NPSG can still bloom in the summer, in some instances annually. Nearly all reported blooms occurring in the eastern region and close to the Hawaiian islands (Calil et al., 2011; Wilson et al., 2013), and rarely reported in the western region (Chow et al., 2017). Suggested mechanisms that may stimulate blooms in the eastern region include shoaling

of the mixed layer (Wilson et al., 2013), eddy interactions (Guidi et al., 2012), mixing at the subtropical front (Wilson & Qiu, 2008), and nitrogen fixation by diazotrophs (Montoya et al., 2004). Along the 30° N latitude line in the northeast Pacific, ocean mixing is influenced by what is referred to as a double critical latitude, where the transformation of internal waves occurs at diurnal and semidiurnal frequencies. These dynamics may interact with areas of weak summer surface stratification near Hawai'i that may facilitate summer phytoplankton blooms across this latitude (Wilson, 2011). Though the biogeochemical interactions throughout the NPSG are dynamically complex, the evidence of higher nutrient availability in the eastern region of the NPSG compared to the western region suggests that phytoplankton growth rates may be elevated in the eastern region for the datasets associated with this research.

2. Objectives and Hypotheses

This research examines the potential drivers of shifts in in situ *Prochlorococcus* growth rates zonally across the NPSG at 30° N. Continuous flow cytometer data and concurrent environmental variables across a transect generates the unique opportunity to investigate the potential driving force of inorganic nutrient composition and flux of nutrient supply on diel shifts in growth rates. Though temperature is recognized as an important driver of *Prochlorococcus* abundance and ecosystem functioning, the data in this research presents a small range of sea surface temperatures across the transect. For this reason, I would like to see how subtle shifts of nutrient influx impacts growth rates. Since the open ocean in the NPSG is oligotrophic, I would expect increased nutrient availability to have a positive relationship with growth rates. Additionally, evidence of increased nutrient availability in the eastern edge of the gyre, and

summertime oceanographic conditions that may lead to phytoplankton blooms, leads me to expect that growth rates would be higher in the eastern side of the transect.

Through this work, I hypothesize:

1. There is a positive correlation between inorganic nutrient availability and the growth rates of *Prochlorococcus*.
2. The eastern region of the north Pacific subtropical gyre produces elevated *Prochlorococcus* growth rates as compared to the western region.

3. Methods

3.1 Field Sampling

FCM data and environmental metrics used in this research were collected from 6 May 2022 to 7 July 2022 during the GO-SHIP cruise P02 aboard the research vessel *Roger Revelle*. This transect followed the 30° north latitude line from offshore Japan (30.49° N, 134.50° E) toward the California coast (30.00° N, 123.09° W). Environmental metrics collected by GO-SHIP on this transect included, but were not limited to, sea surface water temperature and inorganic nutrient composition (NO_3^-, NO_2^-, PO_4^{-3}). The shipboard Cytek Northern Lights spectral FCM continuously collected data on individual pico-nanoplanktonic cells (sized ~0.2-10 μm) from surface waters across the transect.

This transect was broken up into two legs. On the first leg from Guam to Oahu, Hawai'i, (April 30-June 10, 2022) a team member and I collected data for Bio-GO-SHIP, and a separate two person team collected Bio-GO-SHIP data on the second leg from Hawai'i to San Diego,

California (June 12-July 14, 2022) (Figure 1. GO-SHIP P02 Transect, 2022). Once on transect (30° N latitude), scientific collection is a 24-hour operation. One team member works one 12-hour shift, and the remaining 12-hours are completed by the other team member. During my work shift, I maintained the FCM through daily cleanings, calibrations, trouble shooting, and regular observations of data collection for quality control.

Figure 1. GO-SHIP P02 Transect, 2022

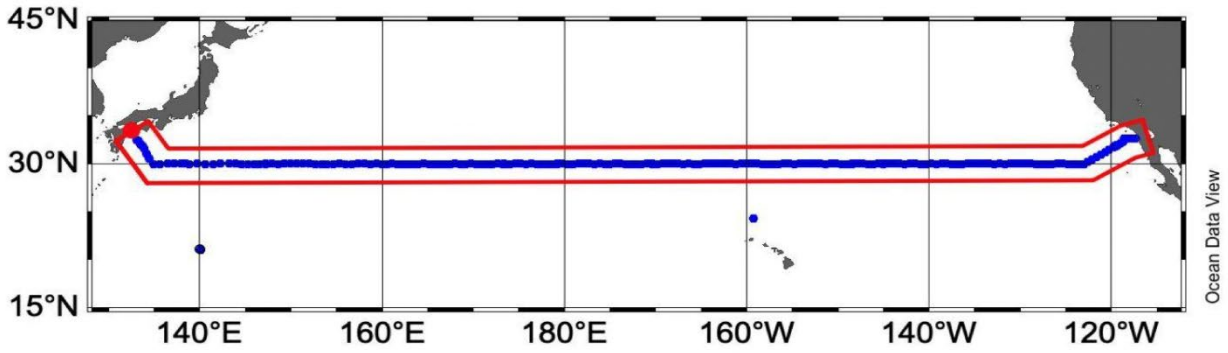

The GO-SHIP P02 transect, completed in the summer of 2022, plotted by Ocean Data View. Blue dots represent sampling stations, with a red outline of the official transect line. Figure courtesy of the Martiny Lab, University of California Irvine.

As part of my duties, I followed additional Bio-GO-SHIP protocols for data collection. This included continuous surface water data of fast repetition rate fluorometry and optical backscattering. Discrete data collection used both underway surface water and water from stations where the ship-based conductivity temperature depth (CTD) system, attached to a Niskin bottle rosette, passed through the entire water column at stations spaced approximately one latitudinal degree apart. Additional discrete data collection that I undertook during the cruise included genetic ‘omics, particulate organic matter, high-performance liquid chromatography, and preserved FCM samples. For each CTD station, the Bio-GO-SHIP team coordinated with

other laboratories on board to appropriately distribute and share water from the Niskin bottles needed for each data analysis. Continuously collected data was stored electronically with back-up systems in place, and discretely collected data was preserved and frozen for later analysis following appropriate protocol. More information on the GO-SHIP and Bio-GO-SHIP P02 protocols can be found in the P02 first leg cruise report: https://cchdo.ucsd.edu/data/35206/33RR20220430_do.pdf.

3.1.1 Environmental Metrics

Underway measurements of surface water temperature were collected through a mounted near-surface thermosalinograph and merged with the FCM dataset based on the closest date and time match. Information regarding these sensors and data collection can be found at https://scripps.ucsd.edu/system/files/2023-06/RogerRevelle.ShipHandbook.2023-05-22.pdf. Near-surface inorganic nutrient data was gathered at depth (between 1.7-33.7 m depth) at CTD stations. The Hydrography Manual and Data Acquisition Overview for GO-SHIP can be found here: https://www.go-ship.org/HydroMan.html. This data was merged with the FCM dataset based on the closest date and time match. For the continuous FCM data collected during transit between stations, these nutrient parameters were merged to the FCM dataset based on the closest station number to each data point.

The nutricline depth, utilized as a proxy for the diapycnal supply of nutrients to the mixed layer, was estimated via nitrate (NO_3^-) profiles from each station, gathered discretely by the CTD rosette. Nitrate profiles were interpolated at 1 m resolution throughout the top 350 m, and the nutricline depth was identified as the depth where the nitrate concentration was greater than a 1 μmol L^{-1} threshold. The nutricline data was merged with the FCM dataset based on the closest

date and time match. For the continuous FCM data collected during transit between stations, these nutrient parameters were merged to the FCM dataset based on the closest station number to each data point.

3.1.2 Flow Cytometry

The FCM was continuously supplied with underway water through a diaphragm pump system. The diaphragm pump system is shown to limit the damage to small-sized individual cells as they pass through the underway system, as compared to an impeller system (Cetinić et al., 2016). FCMs measure both scatter and fluorescent parameters of individual cells using different laser excitations. SSC is the measurement of visible light that is scattered at 90°. It is often suggested that SSC values are related to cell internal complexity, while FSC values are related to cell size. Although SSC is not as commonly used as an estimate of cell size, this research uses a violet small particle detector for obtaining Violet SSC (V-SSC). The small particle detector optimizes the resolution of particles down to ~0.1 μm in diameter. The shipboard FCM operated on a Cytek SpectroFlo software (https://cytekbio.com/pages/spectro-flo) custom template, where ~120 μL of inline water was processed at 20 minute intervals over each 24-hour period. The FCM can identify *Prochlorococcus* populations via light scattering and fluorescence using both 488 nm (blue) and 405 nm (violet) lasers. These scatter and fluorescent variables are measured on a logarithmic scale as V-SSC and red fluorescence (V12 - indicative of chlorophyll) (Figure 2. Flow Cytometer Plot of *Prochlorococcus* Population).

Figure 2. Flow Cytometer Plot of *Prochlorococcus* Population

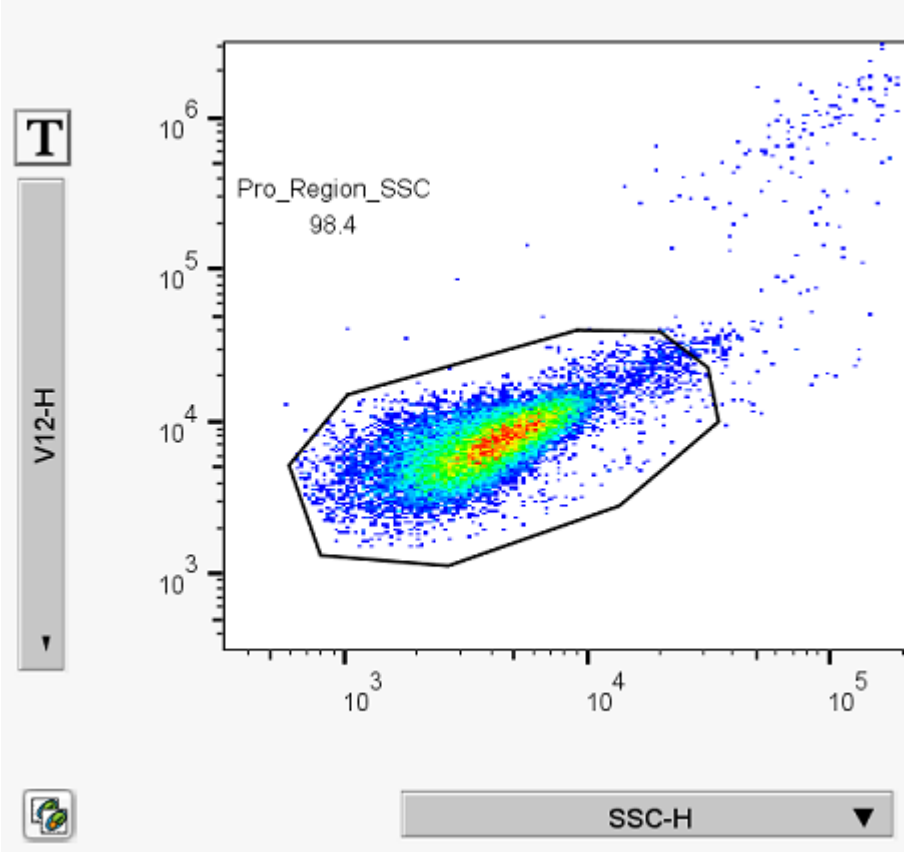

Screen shot image of Prochlorococcus population from the Cytek SpectroFlo software custom template, as detected by a Cytek Northern Lights flow cytometer, in a water sample from the GO-SHIP P02 transect in the summer of 2022. The flow cytometer settings utilize a 408 nm violet laser that can detect particles down to ~0.1 µm in size. The axes are in logarithmic scale, with violet side scatter (SSC-H) on the x-axis, and violet 12 red fluorescence (V12-H) on the y-axis. The black polygon surrounding the Prochlorococcus population represents the gated region. Within this gate is the data that is utilized for analysis.

3.2 Flow Cytometry and Environmental Data Analysis

Raw FCM data from shipboard collection was later processed using FlowJo software V10 (Becton Dickinson, https://www.bdbiosciences.com/en-us/products/software/flowjo-v10-software). The hourly data was partitioned into 24-hour increments, where the first sample plate (36 discrete samples) represented 12-hours, and the second FCM plate represented the remaining 12-hours. Each 12-hour dataset from continuous underway collection was processed in FlowJo

for proper gating of the *Prochlorococcus* populations and the production of data tables and batch graphical visuals. This produced a dataset of V-SSC values for phytoplankton cells at 20 min intervals, partitioned into 12-hour datasets, across the transect. The process of post-cruise processing of FCM data took approximately 90 hours, and I received training and assistance as needed from Nicole Poulton and Laura Lubelczyk of the Center for Aquatic Cytometry at the Bigelow Laboratory for Ocean Sciences. The V-SSC geometric mean of each cell population was converted to cellular carbon content in picograms of carbon (pg C) via a conversion factor calculated from cultured plankton cells (Appendix 1: Side Scatter to Carbon Conversion).

For each diel cycle, the cellular carbon content was plotted over time to visualize the diel oscillations. Apparent sunrise and apparent sunset, which includes the time that light atmospherically refracts before the sun rises on the horizon, and the time after the sunset goes under the horizon but light still is refracted, were included on the plots to assist in the visualizations of diel cell size oscillations. Apparent sunrise and sunset times were calculated utilizing the National Oceanic and Atmospheric Association sunrise/sunset calculator (https://gml.noaa.gov/grad/solcalc/sunrise.html).

The cellular carbon content data was combined with shipboard environmental data based on the date, time, and location of a given data point. For any given data point of cellular carbon content, there are correlated values for sea surface temperature, near-surface inorganic nutrient composition, and interpolated nutricline depth. The continuous cellular carbon content measurements along the 30° N transect were analyzed for statistical significance against the environmental variables by generalized linear modeling.

3.2.1 Sine Modeling for Primary Production per Mean Cell Biomass

Once V-SSC geometric mean values were converted to cellular carbon content, the data was fit to a sine function.

Equation 1:

$$Y = A\sin(t + B) + C$$

$$A = Amplitude\ (\ pg\ C\ )$$

$$B = Offset\ (d)$$

$$C = Mean\ Cell\ Biomass\ (pg\ C)$$

$$t = Time\ (d)$$

$$Y = Carbon\ per\ Cell\ (pg\ C)$$

To fit data into Equation 1, each timepoint was converted to a running time and Equation 1 was then fit to a moving 48-hour window. The moving window timeframe was chosen to accommodate the movement of the ship through differing water masses, while still ensuring there is an appropriate amount of data to fit the model. After fitting data to the sine function, the calculated values of A, B, and C were utilized to calculate primary productivity per mean cell biomass:

Equation 2:

$$Primary\ productivity\ per\ mean\ cell\ biomass\ (d^{-1}) = \frac{(2A)}{C * 1\ day}$$

The amplitude (A) is the distance between the sinusoidal axis and the maximum or minimum peak of the curve. Therefore, 2*A is the distance between the peak and the trough. The

shift of cellular carbon content (Y) from trough to peak, representing carbon assimilation during photosynthesis, is an estimation of the change in cellular carbon content (pg C) over time, which in this case was set to be 1 day (d). Primary production per mean cell biomass (Equation 2) is calculated to estimate how many new *Prochlorococcus* cells can be formed. In order to keep data which exhibited a good fit to the sine function, data was omitted if the associated R^2 values were less than 0.15, and if the modeled growth rate value was greater than 1.4 d^{-1}.

4. Results

4.1 Environmental Trends across Transect

Fifty-three days of data (May 6-July 7, 2022) from the GO-SHIP P02 transect was used for data processing and analysis. Inorganic nutrient concentrations of nitrate, nitrite, and phosphate were very low and therefore not applied in analysis (Table 1. Inorganic Nutrient Compositions). Interpolated nutricline depths, with a minimum value of 32 m and a maximum value of 188 m, generally increased along the transect (Figure 3. Nutricline Depth along P02 Transect). Sea surface temperature, with a minimum value of 18.6 °C and a maximum value of 25.3 °C, gradually increased to ~ 158° W with a local minimum at 174° W, followed by a decrease to the end of the transect (Figure 4. Sea Surface Temperature along P02 Transect).

Table 1. Inorganic Nutrient Compositions

Average Inorganic Nutrient Concentrations	
Nutrient	Average Concentration (µmol/kg)
Nitrate	2.8×10^{-3}
Nitrite	4.60×10^{-4}
Phosphate	0.043

Average inorganic nutrient concentrations gathered over the P02 GO-SHIP transect. More information about this data can be found in section 3.1 Field Sampling.

Figure 3. Nutricline Depth along P02 Transect

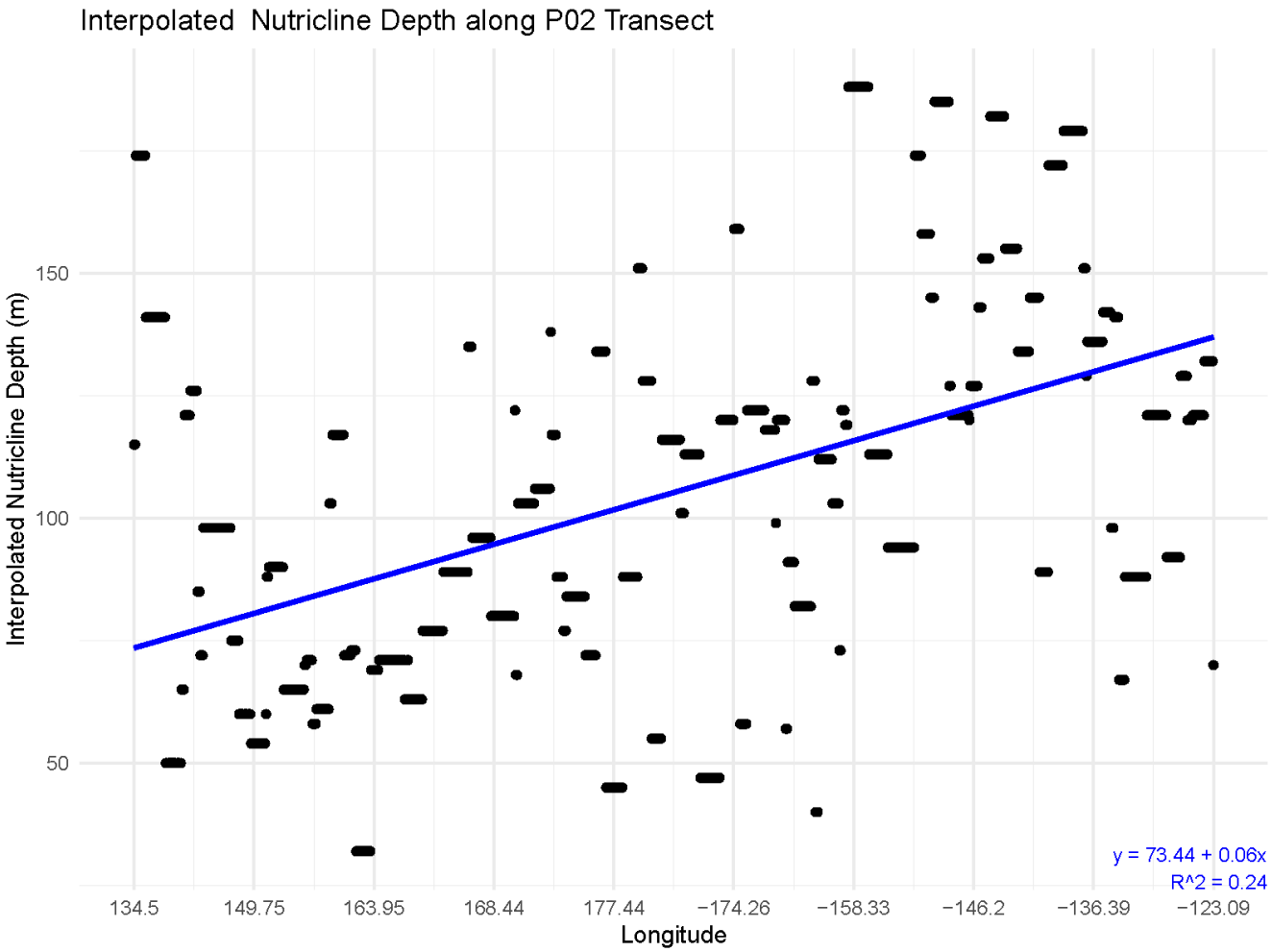

Interpolated nutricline depth (m), derived from nitrate profiles from the 2022 GO-SHIP P02 cruise, plotted over the course of the transect in longitude. The blue line represents the linear regression relationship, with the regression equation and R^2 value labeled in blue text. More information on the interpolation of nutricline depths can be found in section 3.1 Field Sampling.

Figure 4. Sea Surface Temperature along P02 Transect

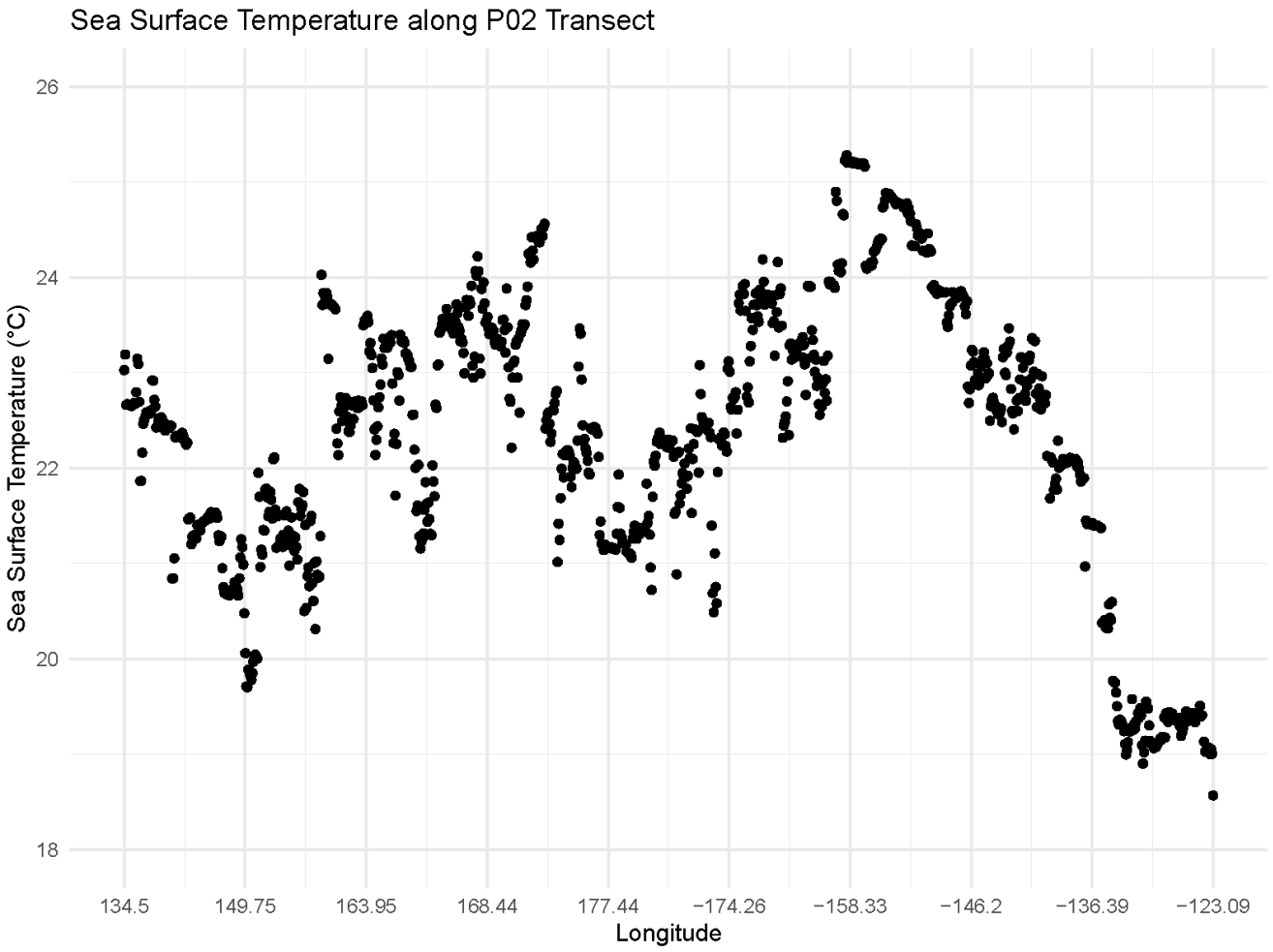

Sea surface temperatures (°C), recorded by a near-surface thermosalinograph during the 2022 GO-SHIP P02 cruise, plotted over the course of the transect in longitude. More information on sampling methods can be found in section 3.1 Field Sampling.

4.2 Cellular Carbon Content and Primary Productivity per Mean Cell Biomass

Cellular carbon content, derived as a linear relationship with V-SSC data (Appendix 1: Side Scatter to Carbon Conversion), shows the diel shifts in cell size throughout the transect. Figure 5. Diel Cycle of Cellular Carbon Content shows the diel cycle from May 20, 2022 at 21:27 UTC, to May 21, 2022 at 04:37 UTC. Cellular carbon content along the transect is depicted in Figure 6. *Prochlorococcus* Cellular Carbon Content along P02 Transect, and values range from 0.0096 - 0.0330 pg C. Modeled primary productivity per mean cell biomass values along the transect is found in Figure 7. *Prochlorococcus* Primary Production per Mean Cell Biomass along P02 Transect, and values range from 0.192- 1.394 d^{-1}.

Figure 5. Diel Cycle of Cellular Carbon Content

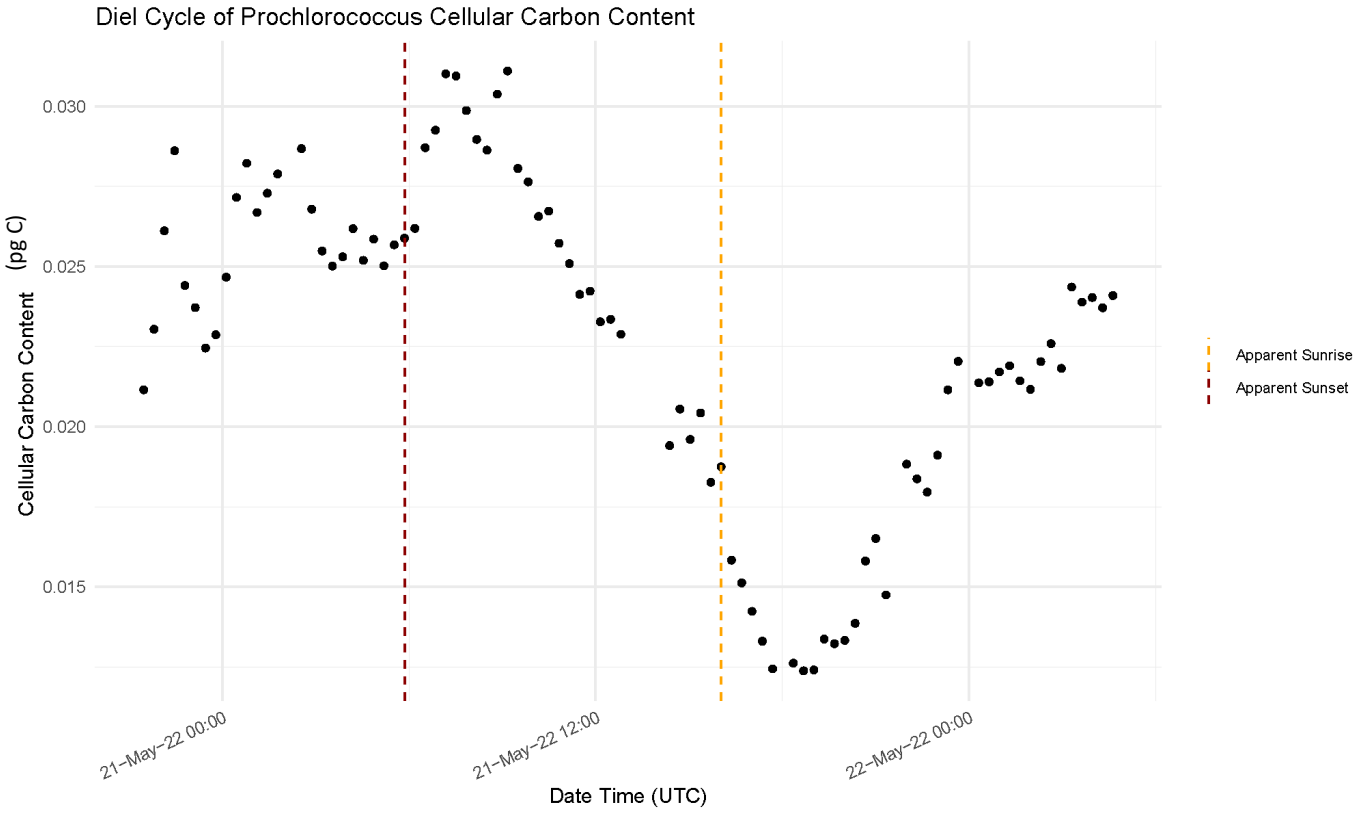

*A diel cycle of cellular carbon content (*pg C*), plotted from May 20, 2022 at 21:27 UTC, to May 21, 2022 at 04:37 UTC. Cellular carbon content is derived from flow cytometer violet side scatter data collected on the 2022 GO-SHIP P02 cruise. The maroon dashed line represents the apparent sunset time, and the yellow dashed line represents the apparent sunrise time. More information on data collection can be found in sections 3.1 Field Sampling and 3.2 Flow Cytometry and Environmental Data Analysis.*

Figure 6. *Prochlorococcus* Cellular Carbon Content along P02 Transect

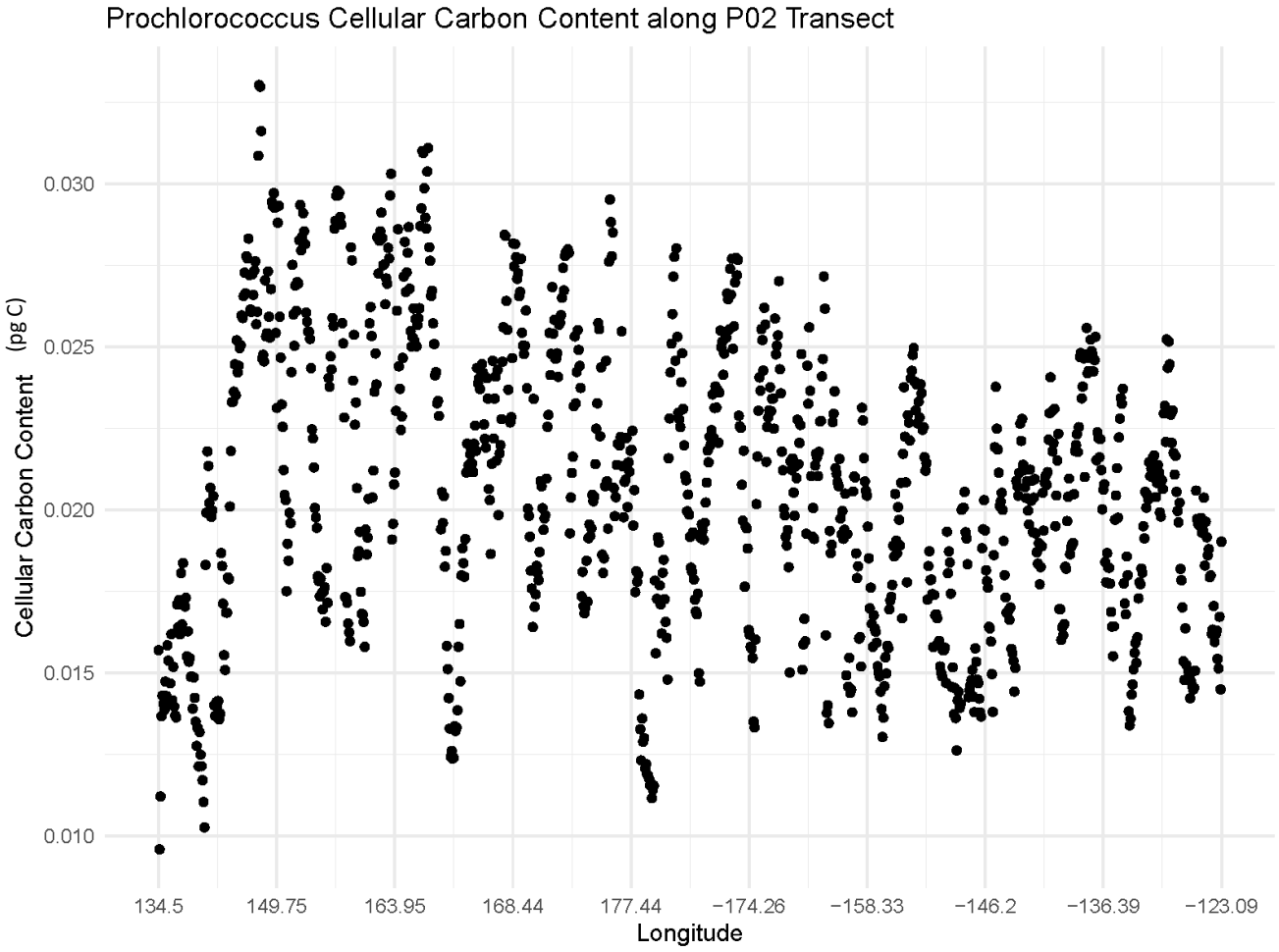

*Cellular carbon content (*pg C*), derived from flow cytometer violet side scatter data collected on the 2022 GO-SHIP P02 cruise, plotted over the course of the transect in longitude. More information on methodology can be found in section 3.1 Field Sampling and 3.2 Flow Cytometry and Environmental Data Analysis.*

Figure 7. *Prochlorococcus* Primary Production per Mean Cell Biomass along P02 Transect

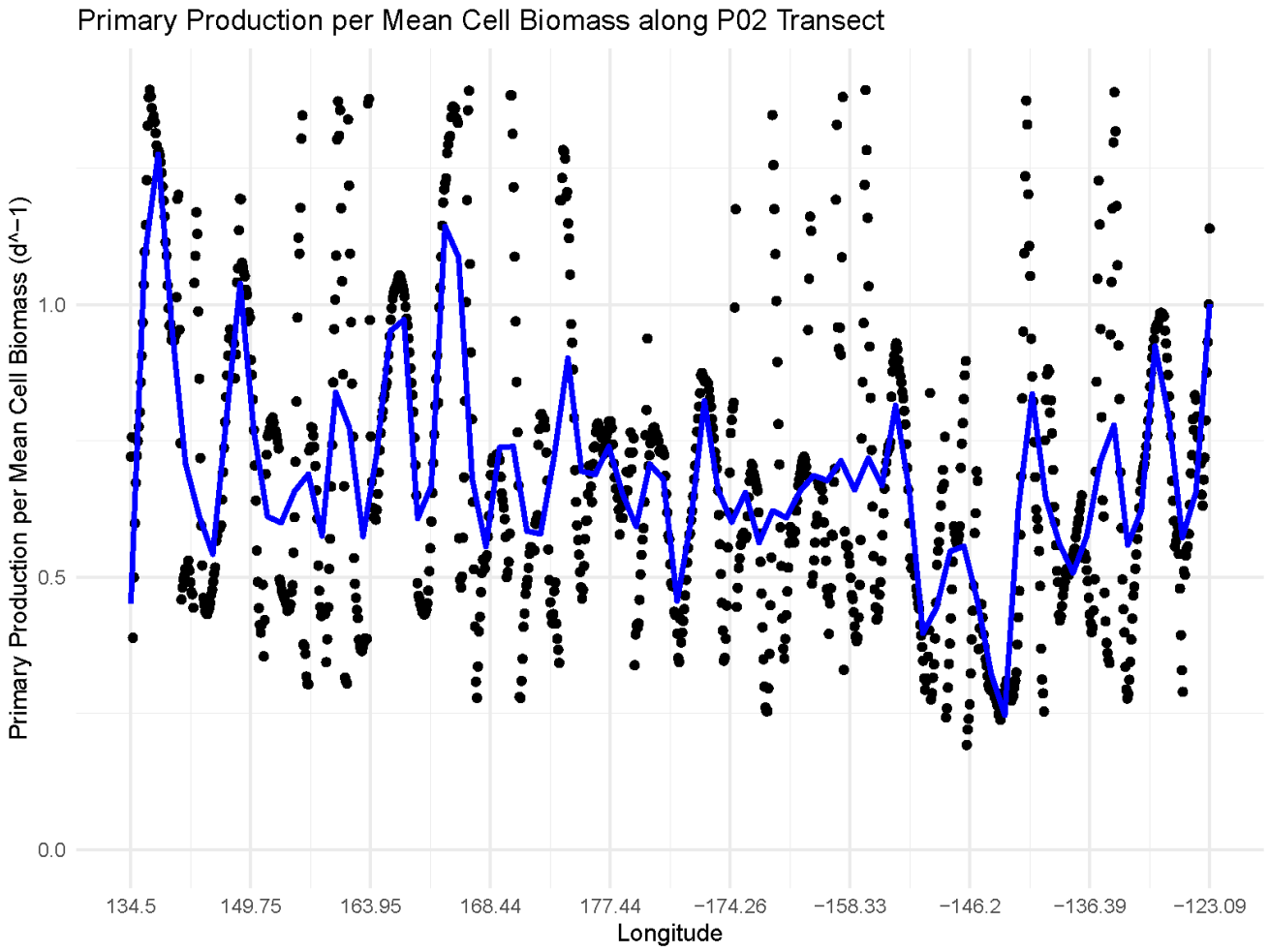

Primary production per mean cell biomass (d^{-1}) of Prochlorococcus, modeled from cellular carbon content data collected during the 2022 GO-SHIP P02 cruise, plotted over the transect in longitude. The blue line represents a LOESS filter of predicted values for visualization. More information on the calculation of primary production values can be found in section 3.2 Flow Cytometry and Environmental Data Analysis.

Prochlorococcus cellular carbon content, run through a general linearized model (GLM), was highly significantly correlated with nutricline depth, and not significantly correlated with sea surface temperature (Table 2. *Prochlorococcus* Cellular Carbon Content Generalized Linear Model Results). When cellular carbon content was run through a two-way GLM, it was highly significantly correlated with both nutricline depth and sea surface temperature (Table 3. *Prochlorococcus* Cellular Carbon Content Two-Way Generalized Linear Model Results, Figure 8. Two-Way Generalized Linear Model Results: Cellular Carbon Content).

Primary production per mean cell biomass, run through a GLM model, was also highly significantly correlated with nutricline depth, but not sea surface temperature (Table 4. *Prochlorococcus* Primary Production per Mean Biomass Generalized Linear Model Results). As a two-way GLM model, primary production per mean cell biomass was significantly correlated only with nutricline depth (Table 5. *Prochlorococcus* Primary Production per Mean Biomass Two-Way Generalized Linear Model Results, Figure 9. Two-Way Generalized Linear Model Results: Primary Production per Mean Cell Biomass).

Table 2. *Prochlorococcus* Cellular Carbon Content Generalized Linear Model Results

Generalized Linear Model						
Independent Variable	Units	Estimate	Standard Error	t Value	Pr (> |t|)	Significance
Nutricline Depth	Meters	-4.190e-05	3.307e-06	-12.672	<2e-16	***
Sea Surface Temperature	° Celsius	9.963e-05	9.153e-05	1.088	0.277	

Generalized linear model results of Prochlorococcus cellular carbon content (pg C) against interpolated nutricline depth (m) and sea surface temperature (°C). All data was collected during the 2022 GO-SHIP P02 cruise. More information on methodology can be found in sections 3.1 Field Sampling and 3.2 Flow Cytometry and Environmental Data Analysis.

Table 3. *Prochlorococcus* Cellular Carbon Content Two-Way Generalized Linear Model Results

Two-Way Generalized Linear Model						
Independent Variable	Units	Estimate	Standard Error	t Value	Pr (> |t|)	Significance
Nutricline Depth	Meters	-4.579e-05	3.421e-06	-13.386	<2e-16	***
Sea Surface Temperature	° Celsius	3.723e-04	8.716e-05	4.271	2.110e-05	***

Two-way generalized linear model results of Prochlorococcus cellular carbon content (pg C) against interpolated nutricline depth (m) and sea surface temperature (°C). All data was collected during the 2022 GO-SHIP P02 cruise. More information on methodology can be found in sections 3.1 Field Sampling and 3.2 Flow Cytometry and Environmental Data Analysis.

Table 4. *Prochlorococcus* Primary Production per Mean Biomass Generalized Linear Model Results

Generalized Linear Model						
Independent Variable	Units	Estimate	Standard Error	t Value	Pr (> |t|)	Significance
Nutricline Depth	Meters	-1.429e-03	2.145e-04	-6.661	4.298e-11	***
Sea Surface Temperature	° Celsius	-7.769e-03	5.641e-03	-1.377	0.169	

Generalized linear model results of Prochlorococcus primary production per mean cell biomass (d^{-1}) against interpolated nutricline depth (m) and sea surface temperature (°C). All data was collected during the 2022 GO-SHIP P02 cruise. More information on methodology can be found in sections 3.1 Field Sampling and 3.2 Flow Cytometry and Environmental Data Analysis.

Table 5. *Prochlorococcus* Primary Production per Mean Biomass Two-Way Generalized Linear Model Results

Two-Way Generalized Linear Model						
Independent Variable	Units	Estimate	Standard Error	t Value	Pr (> |t|)	Significance
Nutricline Depth	Meters	-1.435e-03	2.235e-04	- 6.421	2.030e-10	***
Sea Surface Temperature	° Celsius	7.793e-04	5.696e-03	0.137	0.891	

Two-way generalized linear model results of Prochlorococcus primary production per mean cell biomass (d^{-1}) against interpolated nutricline depth (m) and sea surface temperature (°C). All data was collected during the 2022 GO-SHIP P02 cruise. More information on methodology can be found in sections 3.1 Field Sampling and 3.2 Flow Cytometry and Environmental Data Analysis.

Figure 8. Two-Way Generalized Linear Model Results: Cellular Carbon Content

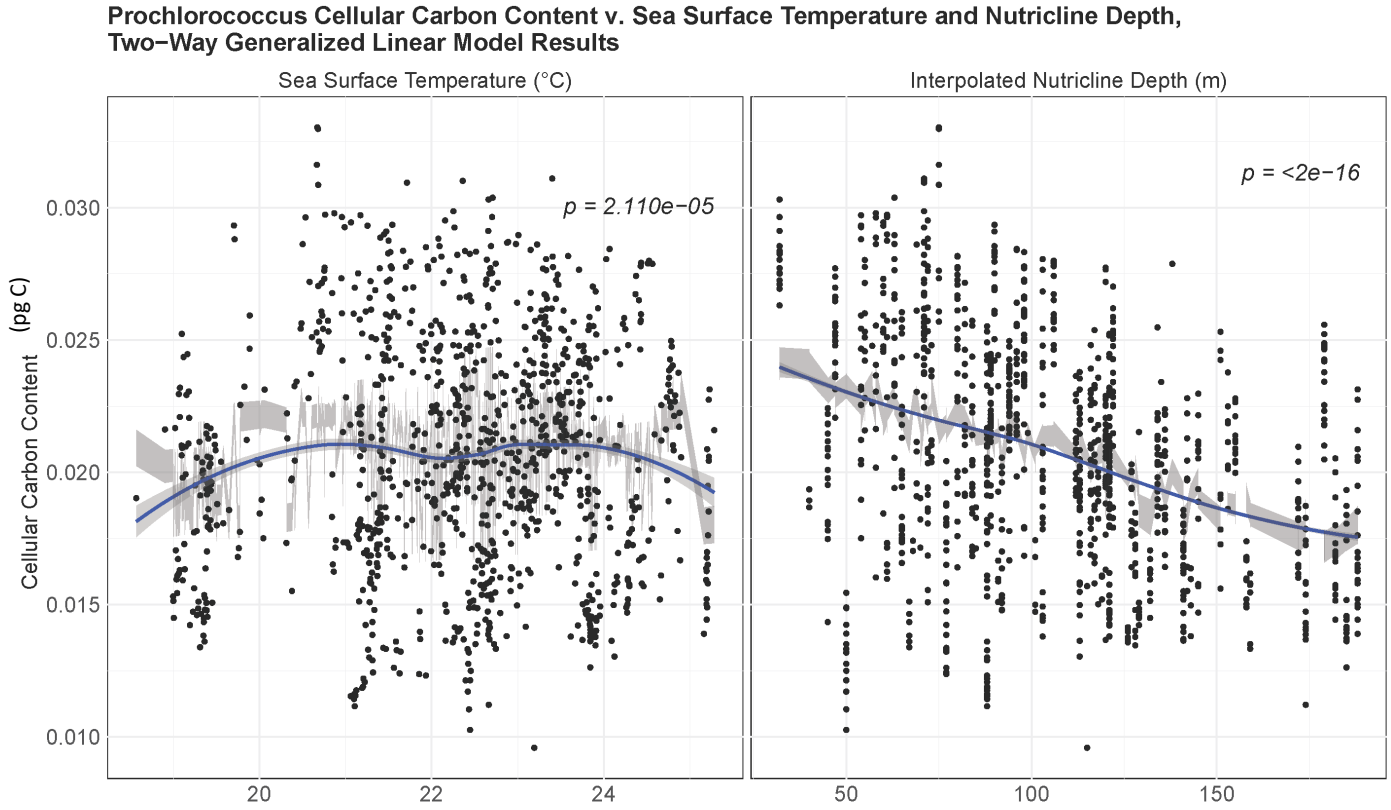

Two-way generalized linear model results of cellular carbon content (pg C) of Prochlorococcus against sea surface temperature (°C) and interpolated nutricline depth (m). Cellular carbon content is derived from flow cytometer violet side scatter data. All parameters were gathered during the summer 2022 GO-SHIP P02 cruise. More information on this methodology can be found in sections 3.1 Field Sampling and 3.2 Flow Cytometry and Environmental Data Analysis. Detailed statistical analysis can be found in Table 3. Prochlorococcus Cellular Carbon Content Two-Way Generalized Linear Model Results. The blue line represents a smoothed LOESS filter of predicted values for visualization. The grey ribbon represents 95% confidence interval around LOESS predicted values (without smoothing). P values, representing data significance, are included for each independent parameter.

Figure 9. Two-Way Generalized Linear Model Results: Primary Production per Mean Cell Biomass

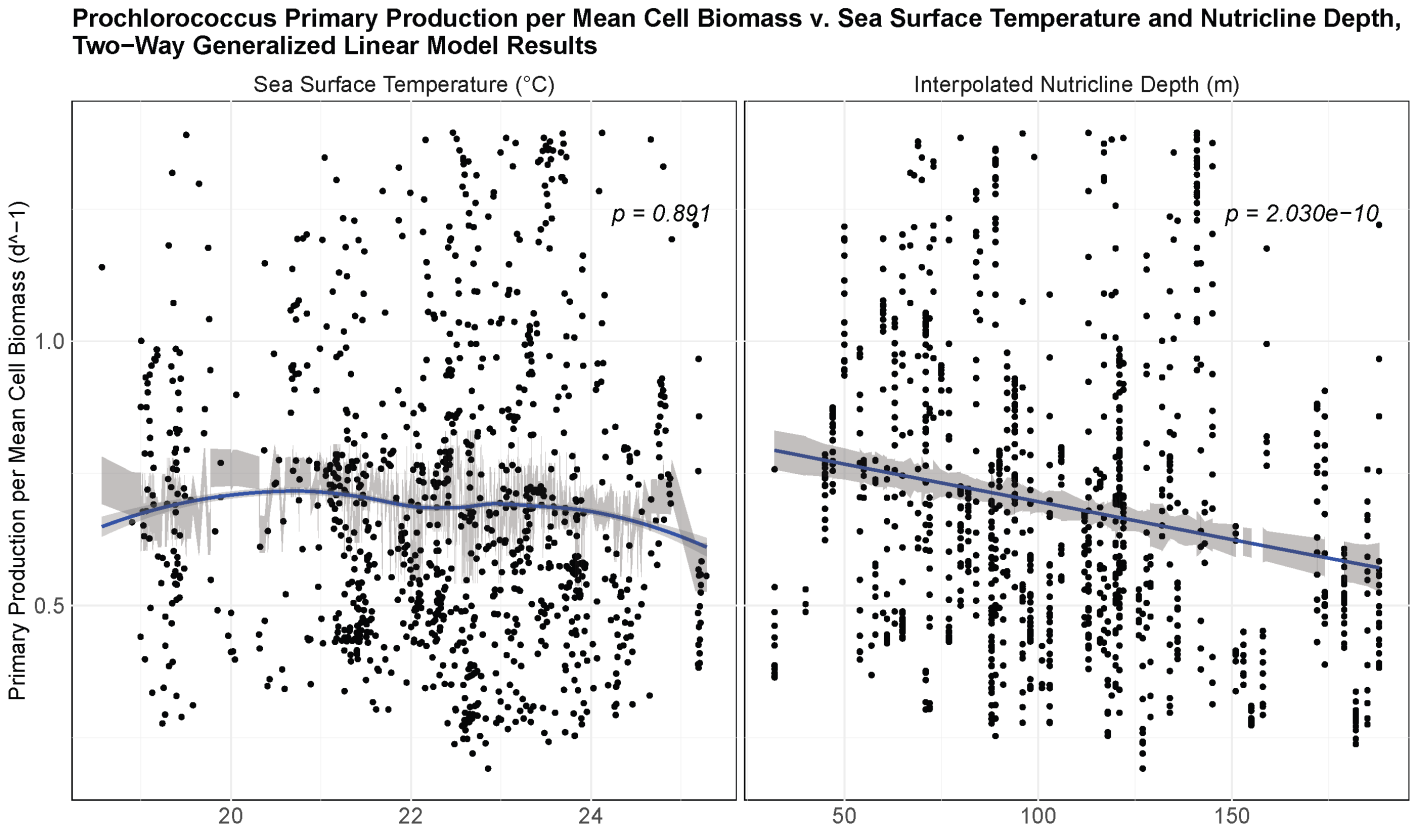

Two-way generalized linear model results of primary production per mean cell biomass (d^{-1}) of Prochlorococcus against sea surface temperature (°C) and interpolated nutricline depth (m). Primary production per mean cell biomass is modeled from flow cytometer violet side scatter data. All parameters were gathered during the summer 2022 GO-SHIP P02 cruise. More information on this methodology can be found in sections 3.1 Field Sampling and 3.2 Flow Cytometry and Environmental Data Analysis. Detailed statistical analysis can be found in Table 5. Prochlorococcus Primary Production per Mean Biomass Two-Way Generalized Linear Model Results. The blue line represents a smoothed LOESS filter of predicted values for visualization. The grey ribbon represents 95% confidence interval around LOESS predicted values (without smoothing). P values, representing data significance, are included for each independent parameter.

5. Discussion

This data was collected in the summer of 2022, following the 30° N latitude line across the NPSG. Patterns in the diel shifts in cellular carbon content of *Prochlorococcus*, as derived from continuous V-SSC data, show growth of individual cell biomass during daylight hours and decrease in cell biomass after sunset (Figure 5. Diel Cycle of Cellular Carbon Content). This agrees with previous observations light-driven diel oscillations noted for cyanobacteria (Ribalet et al., 2015; Sosik et al., 2003; Vaulot & Marie, 1999).

General trends with cellular carbon content show a relationship between cell biomass and nutrient availability; decreased nutrient availability led to smaller *Prochlorococcus* cells (Figure 8. Two-Way Generalized Linear Model Results: Cellular Carbon Content), and decreased growth rates (Figure 9. Two-Way Generalized Linear Model Results: Primary Production per Mean Cell Biomass). The pattern of decreased cell biomass with less nutrient availability is an interesting pattern when considering relationships between cell-surface-to-volume ratio. This increase of cell surface with smaller cell size optimizes the absorption of incident photons (Dufresne et al., 2005). In the most nutrient-poor surface waters of the world, high light adapted ecotypes of *Prochlorococcus* dominate. Additionally, the genomes of these ecotypes are streamlined as compared to other ecotypes. This minimalism of genomic content allows for relative ease of cell propagation in nutrient deplete environments (Partensky & Garczarek, 2010).

Though sea surface temperature was significantly correlated with cellular carbon content (Table 3. *Prochlorococcus* Cellular Carbon Content Two-Way Generalized Linear Model Results), the trend is highly variable. The availability of nutrients is more significant in this research, which is seen in all GLMs. It was expected that, within the oligotrophic waters and small range of sea surface temperatures within the gyre, shifts in nutrient availability would be a

significant driver of growth rates. The results agree with hypothesis #1: increased availability of nutrients, through the shoaling of the nutricline, led to higher growth rates. However, it is fair to debate the biological significance of these findings with the lack of a more robust modeling process, such as a size structured matrix population model with cell abundance data, which I will delve into more shortly.

When considering trends across the NPSG, Figure 4. Sea Surface Temperature along P02 Transect depicts trends unique to gyres. Generally, temperatures decrease at the fringes of the gyre, and there is a decrease of temperature at the dynamic center of a gyre. This is due to wind patterns and the Coriolis effect on the swirling gyre, where Coriolis-driven deflection of water from the fringes toward the center of the gyre forces downwelling at the gyre's center. Figure 4 gives visualization to these trends, with temperature increases at the fringes roughly between longitudes 149° E to 168° E, and from 130° W to 158°W. When examining the eastern and western-most edges of the sea surface temperatures, occurring from roughly longitudes 134° E to 149° E, and from 130° W to 123° W, perhaps these areas are environmental dynamics just outside of the physical gyre. The eastern edge would be dominated by the California Current system.

It was expected that growth rates would be elevated in the eastern region of the NPSG, as compared to the western region. The results of this research disagree with this, with general trends of decreased nutrient availability moving east (Figure 3. Nutricline Depth along P02 Transect), and a negative relationship between nutrient availability and growth rates (Figure 8. Two-Way Generalized Linear Model Results: Cellular Carbon Content). Hypothesis #2 was generated through evidence of increased, transient nutrient availability in the eastern side of the gyre. Nearly all reported blooms of ephemeral increased chlorophyll are noted to occur in the

eastern region of the gyre and close to the Hawaiian islands (Calil et al., 2011; Wilson et al., 2013). Blooms are rarely reported in the western region (Chow et al., 2017). Shoaling of the mixed layer depth is understood as a mechanism to stimulate phytoplankton blooms in the eastern region of the gyre (Wilson et al., 2013). Along the 30° N latitude line in the northeast Pacific, ocean mixing is influenced by what is referred to as a double critical latitude, where the transformation of internal waves occurs at diurnal and semidiurnal frequencies. These dynamics may interact with areas of weak summer surface stratification (facilitated by warmer sea surface temperatures) near Hawai'i that may facilitate summer phytoplankton blooms across this latitude (Wilson, 2011).

The Hawaiian archipelago is situated roughly around the longitudes 178° W and 155° W. Throughout this region, there are some shoaled nutricline depths (Figure 3. Nutricline Depth along P02 Transect), but growth rates are generally quite low (Figure 7. *Prochlorococcus* Primary Production per Mean Cell Biomass along P02 Transect). With phytoplankton blooms being ephemeral, perhaps we did not sail during a bloom event. There are many dynamic and simultaneously occurring environmental variables that may impact phytoplankton growth rates. Investigating more robust modeling results of growth rates compared to additional environmental parameters, such as photosynthetically active radiation, salinity, and acoustic doppler current profiler data, could provide more insight to environmental drivers on shifts in growth rates.

There are some interesting patterns found across the transect. In Figure 10. Noted Patterns along P02 Transect, the olive rectangles highlight a shoaling of nutricline depth, with a concurrent increase of cell biomass, and among the highest growth rates of the transect. The purple rectangles highlight the deepest nutriclines of the transect, with concurrent smaller

and less variable cellular biomass and among the weakest growth rates of the transect. Though some patterns may be noted, the data is quite variable across the transect as a whole.

Figure 10. Noted Patterns along P02 Transect

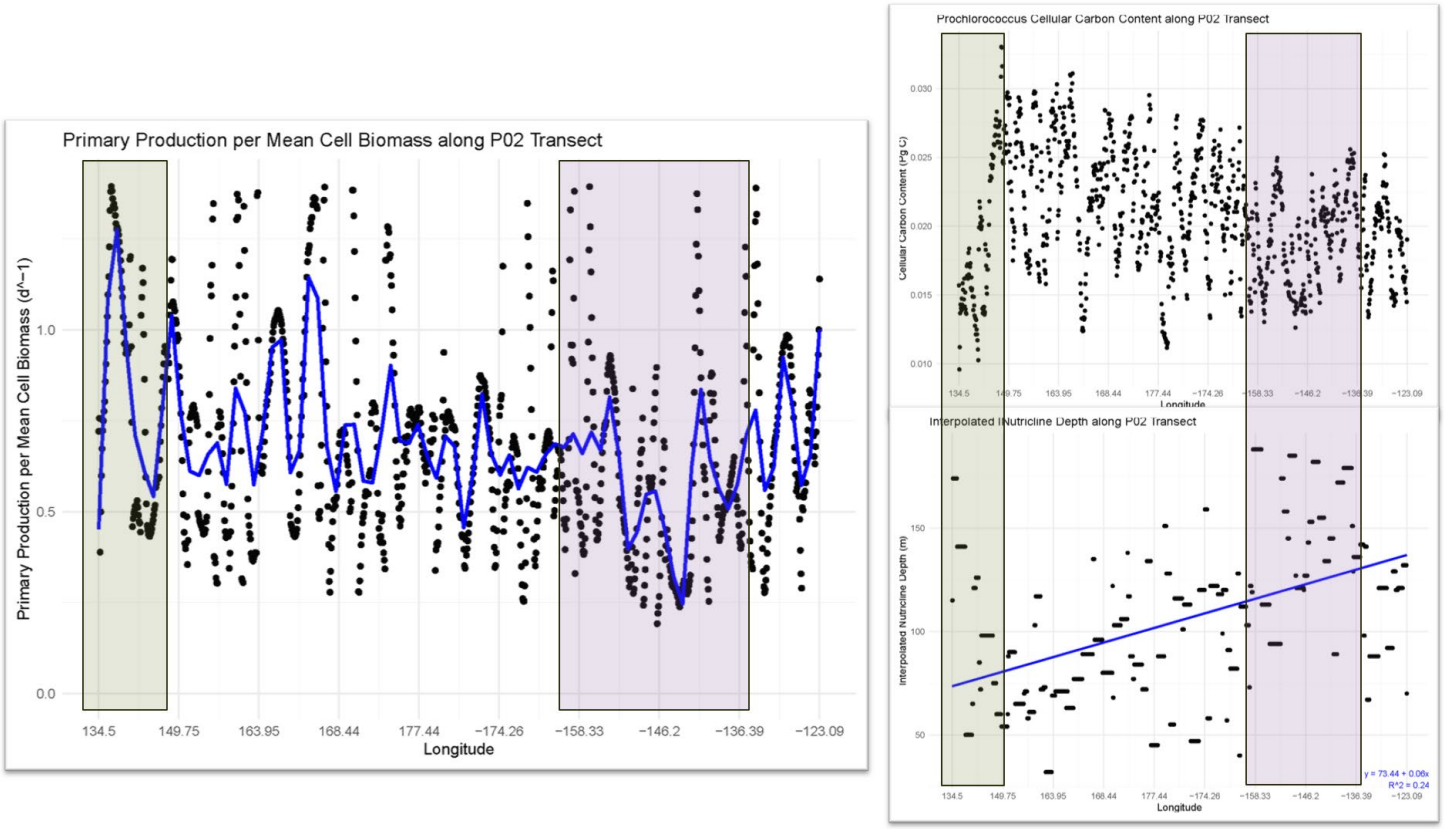

Plots of Prochlorococcus primary production per mean cell biomass, cellular carbon content, and interpolated nutricline depth along the summer 2022 GO-SHIP P02 transect. Reference original figures: Figure 3. Nutricline Depth along P02 Transect, Figure 6. Prochlorococcus Cellular Carbon Content along P02 Transect, Figure 7. Prochlorococcus Primary Production per Mean Cell Biomass along P02 Transect. The olive rectangles and purple rectangles are intended to highlight patterns across the plots, with olive rectangles corresponding to one another, and the same for the purple rectangles.

Another area of interesting patterns is the eastern most edge of this data. Though I do not see patterns of increased nutrients and growth in the eastern region, the eastern edge shows a shoaling of the nutricline and a strengthening of growth rates. Figure 11. Eastern Edge Patterns highlights patterns across nutricline depth, growth rates, and Ocean Data View profiles of inorganic nutrients and water temperature throughout the water column across the P02 transect (figure courtesy of the Martiny Lab, University of California Irvine). As the ship approaches the California coast, I note a shoaling of nutricline depth and an increase of growth rates, which is concurrent with the shoaling of the mixed layer depth as shown in the Ocean Data View plots. The California coastal region is noted for patterns of upwelling that may stimulate phytoplankton growth, though heatwave and climactic patterns may suppress these dynamics (Landry et al., 2024).

Figure 11. Eastern Edge Patterns

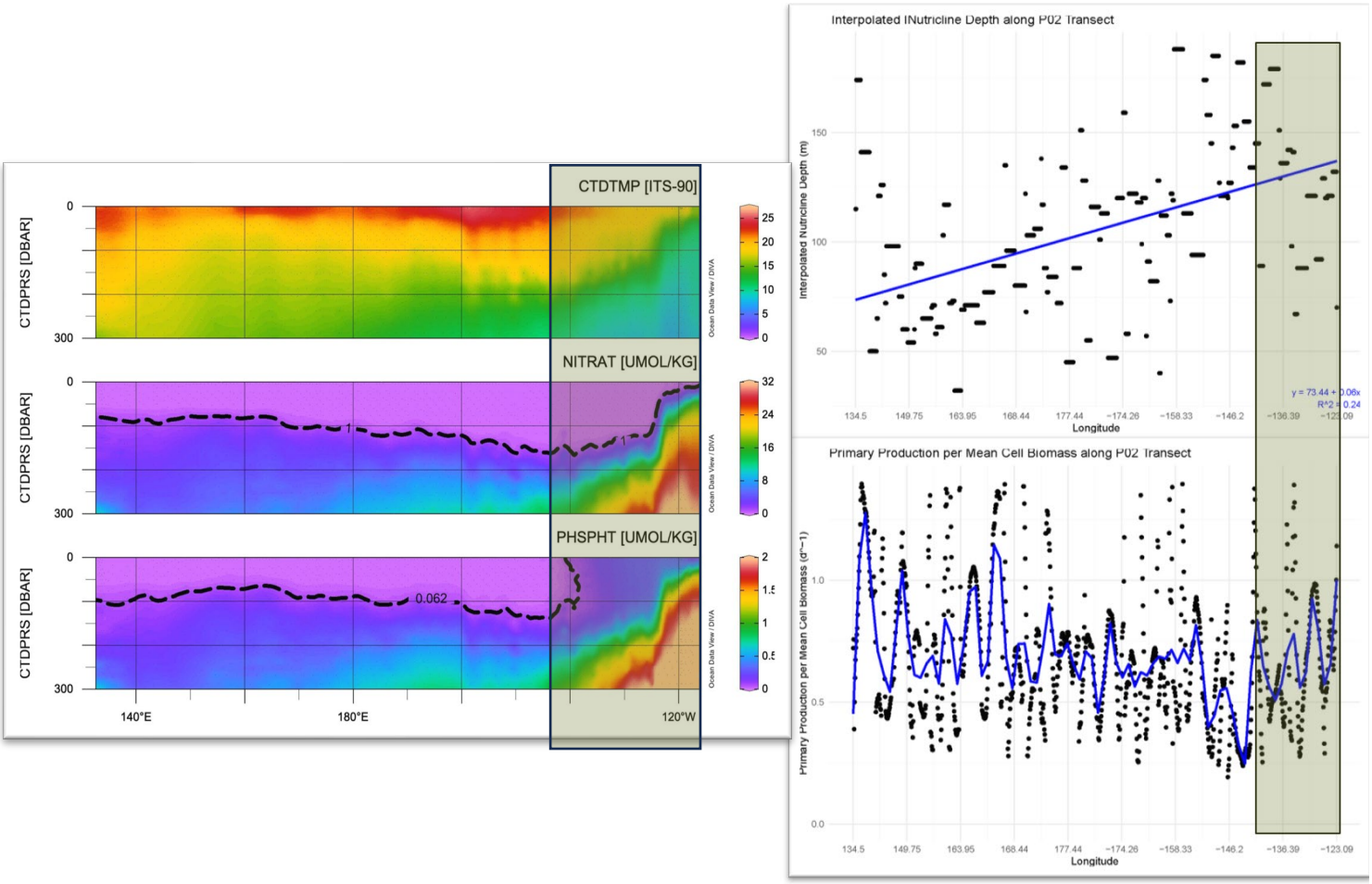

On the right, plots of interpolated nutricline depth and Prochlorococcus primary production per mean cell biomass across the summer 2022 GO-SHIP P02 transect. Reference original figures: Figure 3. Nutricline Depth along P02 Transect, and Figure 7. Prochlorococcus Primary Production per Mean Cell Biomass along P02 Transect. On the left, Ocean Data View plots of 2022 GO-SHIP P02 inorganic nutrient data (nitrate and phosphate, µmol/kilograms), and water temperature (ITS-90) throughout the entire water column across the transect (provided by the Martiny Lab, University of California Irvine). Black dashed lines represent isolines of nitrate (1.0 µmol/kg) and phosphate (0.062 µmol/kg). Olive rectangles are intended to highlight patterns in the data across the figures.

Growth rate values in this research ranged from 0.192- 1.394 d^{-1}. Growth rates of cyanobacteria in the literature, often derived from dilution experiments, tend to vary in the range of 0.2-0.7 d^{-1} (Hunter-Cevera et al., 2014; Worden & Binder, 2003). The most relevant literature to this research is from Ribalet et al. 2015, which modeled division rates in the range of 0.1-0.9 d^{-1}. Though the values from this research may be a bit on the higher edge of the spectrum, the majority of growth rates are situated in the range of ~0.3-0.9 d^{-1}, with a median value of 0.65 d^{-1} (Figure 12. Histogram of *Prochlorococcus* Primary Production per Mean Cell Biomass Values). Though these values modeled through the sine function are within reasonable range, a portion of the data was not a great fit, with small R^2 values and many growth rate values modeled at greater than 1.4 d^{-1}. Values that had R^2 values less than 0.15, or values where modeled growth rate was greater than 1.4 d^{-1}, were omitted from the dataset. This is not ideal, but I worked within feasible limits of my graduation deadlines.

Figure 12. Histogram of *Prochlorococcus* Primary Production per Mean Cell Biomass Values

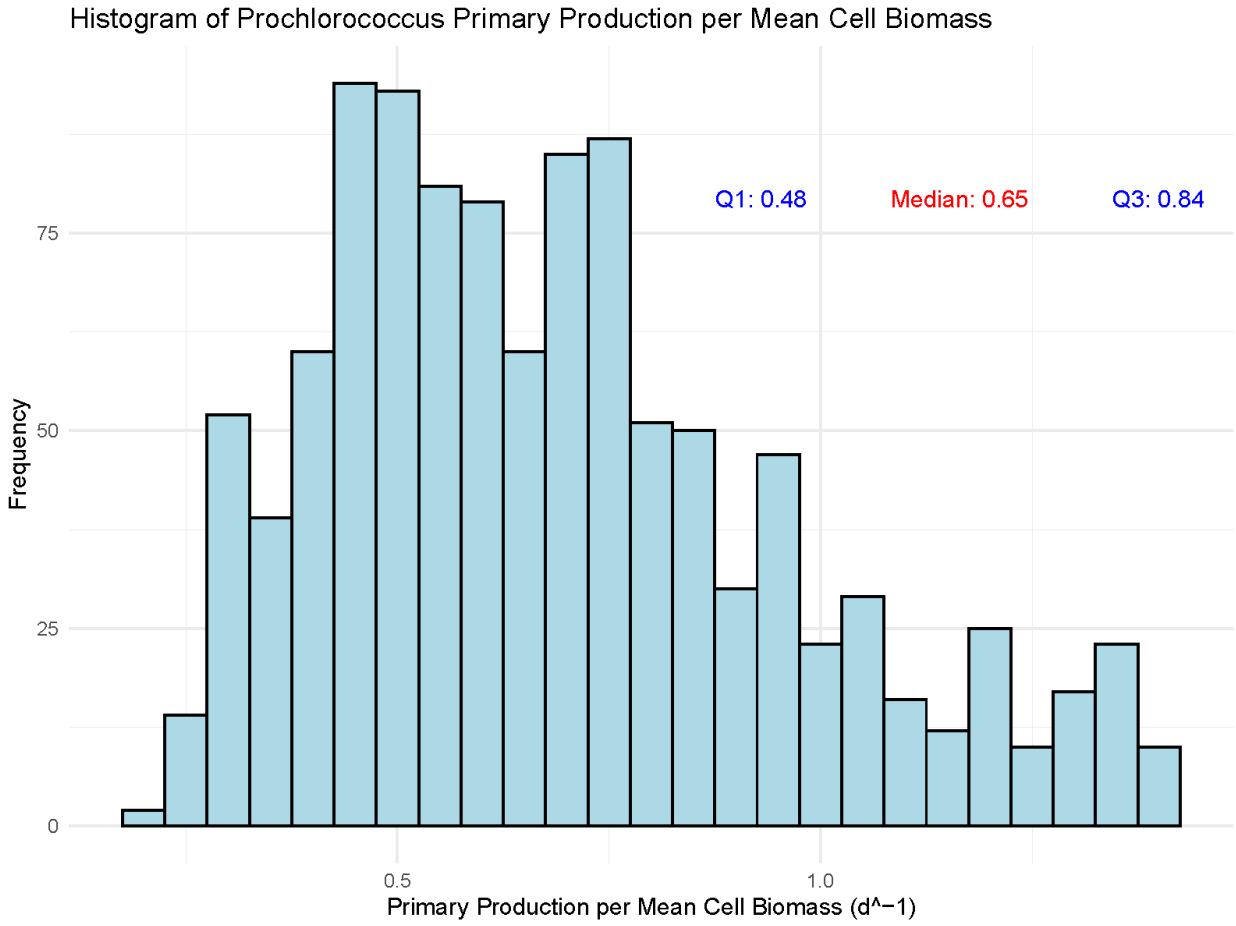

Values of primary production per mean cell biomass (d^{-1}), modeled from cellular carbon content data collected during the 2022 GO-SHIP P02 cruise, plotted as a histogram with quartile values labeled in blue, and median value labeled in red. Reference original data in Figure 7. Prochlorococcus Primary Production per Mean Cell Biomass along P02 Transect.

Currently, the most optimal modeling method for this type of data would be a size-structured matrix population model. Matrix population modeling is dependent on *in situ* abundance and cell-size data over a time series to estimate division and growth rates, and this method has been verified for accuracy with culture experiments (Hunter-Cevera et al., 2014; Ribalet et al., 2015; Sosik et al., 2003). The continuous FCM measurements obtained in this research offer a very high temporal and spatial resolution of diel shifts in cell size across the transect. Additionally, the NPSG, with its minimal range of sea surface temperatures and oligotrophic properties, can be viewed as a natural chemostat. This allows us to investigate changes in modeled growth rates across the transect that may be driven by subtle shifts of nutrient availability or sea surface temperature. This assumption of a closed but continuously refreshed system, driven by the recycling of nutrients through the microbial loop, is necessary for this modeling method. Across more dynamic environments, it is assumed that different populations of *Prochlorococcus* would be sampled. A singular modeling method would not be suitable for differing populations existing in variable environmental conditions.

It was the original goal of this research to use a matrix population model to discern growth rates, but this was not seen to fruition due to time restraints. This model approach, when first introduced as a method for predicting microbial growth rates, was novel in its ability to incorporate the full size distribution of the population, as well as accounting for simultaneous cell growth and division. The size distribution method can determine cell-specific growth rates that are independent of shifts in cell concentration, which allows for the separation of the effects of natural mortality, grazing, viral infection, and mixing of populations via mixing of water masses (Sosik et al., 2003). Once the FCM dataset for this research is modified to depict accurate cell abundance data, we would be able to generate a matrix population model.

Though the optimal modeling methodology was not implemented in this research, the sine model provided interesting insight to trends across the transect. At this resolution, nutrient availability appears to be the most significant driver of shifts in *Prochlorococcus* growth rates. The P02 transect was the pilot cruise for the full suite of Bio-GO-SHIP protocols. Through trial and error, this cruise provided a great starting point for the standardization of data collection methodologies to understand phytoplankton dynamics at ocean basin scales. Additionally, this thesis project provides a preliminary foundation for the standardization of data analysis with FCM data.

References

Anderson, R., Archer, D., Bathmann, U., Boyd, P., Buesseler, K., Burkill, P., Bychkov, A., Carlson, C., Chen, C.-T. A., & Doney, S. (2001). A new vision of ocean biogeochemistry after a decade of the Joint Global Ocean Flux Study (JGOFS). *Ambio*, *10*, 4.

Behrenfeld, M. (2011). Uncertain future for ocean algae. *Nature Climate Change*, *1*(1), 33–34. https://doi.org/10.1038/nclimate1069

Behrenfeld, M., Boss, E., Siegel, D. A., & Shea, D. M. (2005). Carbon-based ocean productivity and phytoplankton physiology from space: phytoplankton growth rates and ocean productivity. *Global Biogeochemical Cycles*, *19*(1). https://doi.org/10.1029/2004GB002299

Behrenfeld, M., & Boss, E. (2014). Resurrecting the ecological underpinnings of ocean plankton blooms. *Annual Review of Marine Science*, *6*(1), 167–194. https://doi.org/10.1146/annurev-marine-052913-021325

Bender, M., Grande, K., Johnson, K., Marra, J., Williams, P. J. LeB., Sieburth, J., Pilson, M., Langdon, C., Hitchcock, G., Orchardo, J., Hunt, C., Donaghay, P., & Heinemann, K. (1987). A comparison of four methods for determining planktonic community production1: Planktonic community production. *Limnology and Oceanography*, *32*(5), 1085–1098. https://doi.org/10.4319/lo.1987.32.5.1085

Berube, P. M., Biller, S. J., Kent, A. G., Berta-Thompson, J. W., Roggensack, S. E., Roache-Johnson, K. H., Ackerman, M., Moore, L. R., Meisel, J. D., Sher, D., Thompson, L. R., Campbell, L., Martiny, A. C., & Chisholm, S. W. (2015). Physiology and evolution of nitrate acquisition in *Prochlorococcus*. *The ISME Journal*, *9*(5), Article 5. https://doi.org/10.1038/ismej.2014.211

Bohren, C. F., & Huffman, D. R. (1983). *Absorption and scattering of light by small particles*. Wiley-VCH.

Bopp, L., Resplandy, L., Orr, J. C., Doney, S. C., Dunne, J. P., Gehlen, M., Halloran, P., Heinze, C., Ilyina, T., Séférian, R., Tjiputra, J., & Vichi, M. (2013). Multiple stressors of ocean ecosystems in the 21st century: Projections with CMIP5 models. *Biogeosciences*, *10*(10), 6225–6245. https://doi.org/10.5194/bg-10-6225-2013

Bouman, H. A., Ulloa, O., Scanlan, D. J., Zwirglmaier, K., Li, W. K. W., Platt, T., Stuart, V., Barlow, R., Leth, O., Clementson, L., Lutz, V., Fukasawa, M., Watanabe, S., & Sathyendranath, S. (2006). Oceanographic Basis of the Global Surface Distribution of *Prochlorococcus* Ecotypes. *Science*, *312*(5775), 918–921. https://doi.org/10.1126/science.1122692

Calil, P. H. R., Doney, S. C., Yumimoto, K., Eguchi, K., & Takemura, T. (2011). Episodic upwelling and dust deposition as bloom triggers in low-nutrient, low-chlorophyll regions. *Journal of Geophysical Research*, *116*(C6), C06030. https://doi.org/10.1029/2010JC006704

Campbell, L., & Carpenter, E. (1986). Diel patterns of cell division in marine *Synechococcus* spp. (Cyanobacteria): Use of the frequency of dividing cells technique to measure growth rate. *Marine Ecology Progress Series*, *32*, 139–148. https://doi.org/10.3354/meps032139

Caswell, H. (2001). *Matrix population models: Construction, analysis, and interpretation. 2nd edn Sinauer Associates*. Inc., Sunderland, MA.

Cermeño, P., Dutkiewicz, S., Harris, R. P., Follows, M., Schofield, O., & Falkowski, P. G. (2008). The role of nutricline depth in regulating the ocean carbon cycle. *Proceedings of*

the National Academy of Sciences, *105*(51), 20344–20349. https://doi.org/10.1073/pnas.0811302106

Cetinić, I., Poulton, N., & Slade, W. H. (2016). Characterizing the phytoplankton soup: Pump and plumbing effects on the particle assemblage in underway optical seawater systems. *Optics Express*, *24*(18), 20703–20715. https://doi.org/10.1364/OE.24.020703

Chisholm, S. W., Olson, R. J., Zettler, E. R., Goericke, R., Waterbury, J. B., & Welschmeyer, N. A. (1988). A novel free-living prochlorophyte abundant in the oceanic euphotic zone. *Nature*, *334*(6180), 340–343. https://doi.org/10.1038/334340a0

Chow, C. H., Cheah, W., & Tai, J.-H. (2017). A rare and extensive summer bloom enhanced by ocean eddies in the oligotrophic western North Pacific Subtropical Gyre. *Scientific Reports*, *7*(1), 6199. https://doi.org/10.1038/s41598-017-06584-3

Chow, C. H., Cheah, W., Tai, J.-H., & Liu, S.-F. (2019). Anomalous wind triggered the largest phytoplankton bloom in the oligotrophic North Pacific Subtropical Gyre. *Scientific Reports*, *9*(1), Article 1. https://doi.org/10.1038/s41598-019-51989-x

Clayton, S., Alexander, H., Graff, J. R., Poulton, N. J., Thompson, L. R., Benway, H., Boss, E., & Martiny, A. (2022). Bio-GO-SHIP: the time is right to establish global repeat sections of ocean biology. *Frontiers in Marine Science*, *8*. https://www.frontiersin.org/articles/10.3389/fmars.2021.767443

Denman, K. L., & Gargett, A. E. (1983). Time and space scales of vertical mixing and advection of phytoplankton in the upper ocean. *Limnology and Oceanography*, *28*(5), 801–815. https://doi.org/10.4319/lo.1983.28.5.0801

Dubelaar, G. B. J., Gerritzen, P. L., Beeker, A. E. R., Jonker, R. R., & Tangen, K. (1999). Design and first results of CytoBuoy: A wireless flow cytometer for in situ analysis of marine

and fresh waters. *Cytometry*, *37*(4), 247–254. https://doi.org/10.1002/(SICI)1097-0320(19991201)37:4<247::AID-CYTO1>3.0.CO;2-9

Dufresne, A., Garczarek, L., & Partensky, F. (2005). Accelerated evolution associated with genome reduction in a free-living prokaryote. *Genome Biology*, *6*(2), R14. https://doi.org/10.1186/gb-2005-6-2-r14

DuRand, M. D. (1995). *Phytoplankton growth and diel variations in beam attenuation through individual cell analysis*. Massachusetts Institute of Technology and Woods Hole Oceanographic Institution. https://doi.org/10.1575/1912/5616

Endo, H., & Suzuki, K. (2019). Spatial variations in community structure of haptophytes across the kuroshio front in the tokara strait. In T. Nagai, H. Saito, K. Suzuki, & M. Takahashi (Eds.), *Geophysical Monograph Series* (1st ed., pp. 207–221). Wiley. https://doi.org/10.1002/9781119428428.ch13

Eppley, R. W., & Peterson, B. J. (1979). Particulate organic matter flux and planktonic new production in the deep ocean. *Nature*, *282*(5740), Article 5740. https://doi.org/10.1038/282677a0

Fenchel, T. (1988). Marine Plankton Food Chains. *Annual Review of Ecology and Systematics*, *19*(1), 19–38. https://doi.org/10.1146/annurev.es.19.110188.000315

Field, C. B., Behrenfeld, M. J., Randerson, J. T., & Falkowski, P. (1998). Primary production of the biosphere: integrating terrestrial and oceanic components. *Science*, *281*(5374), 237–240. https://doi.org/10.1126/science.281.5374.237

Flombaum, P., Gallegos, J. L., Gordillo, R. A., Rincón, J., Zabala, L. L., Jiao, N., Karl, D. M., Li, W. K. W., Lomas, M. W., Veneziano, D., Vera, C. S., Vrugt, J. A., & Martiny, A. C. (2013). Present and future global distributions of the marine cyanobacteria

Prochlorococcus and *Synechococcus*. *Proceedings of the National Academy of Sciences*, *110*(24), 9824–9829. https://doi.org/10.1073/pnas.1307701110

Fu, W., Randerson, J. T., & Moore, J. K. (2016). Climate change impacts on net primary production (NPP) and export production (EP) regulated by increasing stratification and phytoplankton community structure in the CMIP5 models. *Biogeosciences*, *13*(18), 5151–5170. https://doi.org/10.5194/bg-13-5151-2016

Gallegos, C. L. (1989). Microzooplankton grazing on phytoplankton in the Rhode River, Maryland: Nonlinear feeding kinetics. *Marine Ecology Progress Series*, *57*, 22–33.

Geider, R. J. (1987). Light and temperature dependence of the carbon to chlorophyll a ratio in microalgae and cyanobacteria: implications for physiology and growth of phytoplankton. *The New Phytologist*, *106*(1), 1–34.

Guidi, L., Calil, P. H. R., Duhamel, S., Björkman, K. M., Doney, S. C., Jackson, G. A., Li, B., Church, M. J., Tozzi, S., Kolber, Z. S., Richards, K. J., Fong, A. A., Letelier, R. M., Gorsky, G., Stemmann, L., & Karl, D. M. (2012). Does eddy-eddy interaction control surface phytoplankton distribution and carbon export in the North Pacific Subtropical Gyre? *Journal of Geophysical Research: Biogeosciences*, *117*(G2), 2012JG001984. https://doi.org/10.1029/2012JG001984

Hagström, Å., Azam, F., Andersson, A., Wikner, J., & Rassoulzadegan, F. (1988). Microbial loop in an oligotrophic pelagic marine ecosystem: Possible roles of cyanobacteria and nanoflagellates in the organic fluxes. *Marine Ecology Progress Series*, *49*, 171–178. https://doi.org/10.3354/meps049171

Hagström, Larsson, U., Hörstedt, P., & Normark, S. (1979). Frequency of dividing cells, a new approach to the determination of bacterial growth rates in aquatic environments. *Applied*

and Environmental Microbiology, *37*(5), 805–812. https://doi.org/10.1128/aem.37.5.805-812.1979

Hu, D., Wu, L., Cai, W., Gupta, A. S., Ganachaud, A., Qiu, B., Gordon, A. L., Lin, X., Chen, Z., Hu, S., Wang, G., Wang, Q., Sprintall, J., Qu, T., Kashino, Y., Wang, F., & Kessler, W. S. (2015). Pacific western boundary currents and their roles in climate. *Nature*, *522*(7556), 299–308. https://doi.org/10.1038/nature14504

Hunter-Cevera, K. R., Neubert, M. G., Olson, R. J., Shalapyonok, A., Solow, A. R., & Sosik, H. M. (2020). Seasons of Syn. *Limnology and Oceanography*, *65*(5), 1085–1102. https://doi.org/10.1002/lno.11374

Hunter-Cevera, K. R., Neubert, M. G., Olson, R. J., Solow, A. R., Shalapyonok, A., & Sosik, H. M. (2016). Physiological and ecological drivers of early spring blooms of a coastal phytoplankter. *Science*, *354*(6310), 326–329. https://doi.org/10.1126/science.aaf8536

Hunter-Cevera, K. R., Neubert, M. G., Solow, A. R., Olson, R. J., Shalapyonok, A., & Sosik, H. M. (2014). Diel size distributions reveal seasonal growth dynamics of a coastal phytoplankter. *Proceedings of the National Academy of Sciences*, *111*(27), 9852–9857. https://doi.org/10.1073/pnas.1321421111

Krumhardt, K. M., Long, M. C., Sylvester, Z. T., & Petrik, C. M. (2022). Climate drivers of Southern Ocean phytoplankton community composition and potential impacts on higher trophic levels. *Frontiers in Marine Science*, *9*. https://www.frontiersin.org/articles/10.3389/fmars.2022.916140

Landry, M. R., Freibott, A. L., Stukel, M. R., Selph, K. E., Allen, A. E., & Rabines, A. (2024). Phytoplankton growth and grazing dynamics during anomalous heat wave and suppressed

upwelling conditions in the southern California Current. *Deep Sea Research Part I: Oceanographic Research Papers*, *210*, 104353. https://doi.org/10.1016/j.dsr.2024.104353

Landry, M. R., & Hassett, R. P. (1982). Estimating the grazing impact of marine micro-zooplankton. *Marine Biology*, *67*(3), 283–288. https://doi.org/10.1007/BF00397668

Lange, P. K., Brewin, R. J. W., Dall'Olmo, G., Tarran, G. A., Sathyendranath, S., Zubkov, M., & Bouman, H. A. (2018). Scratching beneath the surface: a model to predict the vertical distribution of *Prochlorococcus* using remote sensing. *Remote Sensing*, *10*(6), Article 6. https://doi.org/10.3390/rs10060847

Larkin, A. A., Blinebry, S. K., Howes, C., Lin, Y., Loftus, S. E., Schmaus, C. A., Zinser, E. R., & Johnson, Z. I. (2016). Niche partitioning and biogeography of high light adapted *Prochlorococcus* across taxonomic ranks in the North Pacific. *The ISME Journal*, *10*(7), 1555–1567. https://doi.org/10.1038/ismej.2015.244

Larkin, A. A., Garcia, C. A., Ingoglia, K. A., Garcia, N. S., Baer, S. E., Twining, B. S., Lomas, M. W., & Martiny, A. C. (2020). Subtle biogeochemical regimes in the Indian Ocean revealed by spatial and diel frequency of *Prochlorococcus* haplotypes. *Limnology and Oceanography*, *65*(S1), S220–S232. https://doi.org/10.1002/lno.11251

Larkin, A. A., Hagstrom, G. I., Brock, M. L., Garcia, N. S., & Martiny, A. C. (2023). Basin-scale biogeography of *Prochlorococcus* and SAR11 ecotype replication. *The ISME Journal*, *17*(2), Article 2. https://doi.org/10.1038/s41396-022-01332-6

Liu, H., Nolla, H., & Campbell, L. (1997). *Prochlorococcus* growth rate and contribution to primary production in the equatorial and subtropical North Pacific Ocean. *Aquatic Microbial Ecology*, *12*(1), 39–47. https://doi.org/10.3354/ame012039

Liu, K., Suzuki, K., Chen, B., & Liu, H. (2021). Are temperature sensitivities of *Prochlorococcus* and Synechococcus impacted by nutrient availability in the subtropical northwest Pacific? *Limnology and Oceanography*, *66*(3), 639–651. https://doi.org/10.1002/lno.11629

Malmstrom, R. R., Coe, A., Kettler, G. C., Martiny, A. C., Frias-Lopez, J., Zinser, E. R., & Chisholm, S. W. (2010). Temporal dynamics of *Prochlorococcus* ecotypes in the Atlantic and Pacific oceans. *The ISME Journal*, *4*(10), Article 10. https://doi.org/10.1038/ismej.2010.60

Mann, K. H., & Lazier, J. R. N. (2006). *Dynamics of marine ecosystems: Biological-physical interactions in the oceans* (3rd ed). Blackwell Pub.

Marañón, E., Lorenzo, M. P., Cermeño, P., & Mouriño-Carballido, B. (2018). Nutrient limitation suppresses the temperature dependence of phytoplankton metabolic rates. *The ISME Journal*, *12*(7), Article 7. https://doi.org/10.1038/s41396-018-0105-1

Martiny, A. C., Hagstrom, G. I., DeVries, T., Letscher, R. T., Britten, G. L., Garcia, C. A., Galbraith, E., Karl, D., Levin, S. A., Lomas, M. W., Moreno, A. R., Talmy, D., Wang, W., & Matsumoto, K. (2022). Marine phytoplankton resilience may moderate oligotrophic ecosystem responses and biogeochemical feedbacks to climate change. *Limnology and Oceanography*, *67*(S1), S378–S389. https://doi.org/10.1002/lno.12029

Martiny, A. C., Huang, Y., & Li, W. (2009). Occurrence of phosphate acquisition genes in *Prochlorococcus* cells from different ocean regions. *Environmental Microbiology*, *11*(6), 1340–1347. https://doi.org/10.1111/j.1462-2920.2009.01860.x

Martiny, A. C., Kathuria, S., & Berube, P. M. (2009). Widespread metabolic potential for nitrite and nitrate assimilation among *Prochlorococcus* ecotypes. *Proceedings of the National Academy of Sciences*, *106*(26), 10787–10792. https://doi.org/10.1073/pnas.0902532106

Martiny, A. C., Ma, L., Mouginot, C., Chandler, J. W., & Zinser, E. R. (2016). Interactions between thermal acclimation, growth rate, and phylogeny influence *Prochlorococcus* elemental stoichiometry. *PLOS ONE*, *11*(12), e0168291. https://doi.org/10.1371/journal.pone.0168291

Mattern, J. P., Glauninger, K., Britten, G. L., Casey, J. R., Hyun, S., Wu, Z., Armbrust, E. V., Harchaoui, Z., & Ribalet, F. (2022). A Bayesian approach to modeling phytoplankton population dynamics from size distribution time series. *PLOS Computational Biology*, *18*(1), e1009733. https://doi.org/10.1371/journal.pcbi.1009733

Miloslavich, P., Bax, N. J., Simmons, S. E., Klein, E., Appeltans, W., Aburto-Oropeza, O., Andersen Garcia, M., Batten, S. D., Benedetti-Cecchi, L., Checkley Jr., D. M., Chiba, S., Duffy, J. E., Dunn, D. C., Fischer, A., Gunn, J., Kudela, R., Marsac, F., Muller-Karger, F. E., Obura, D., & Shin, Y.-J. (2018). Essential ocean variables for global sustained observations of biodiversity and ecosystem changes. *Global Change Biology*, *24*(6), 2416–2433. https://doi.org/10.1111/gcb.14108

Montoya, J. P., Holl, C. M., Zehr, J. P., Hansen, A., Villareal, T. A., & Capone, D. G. (2004). High rates of N2 fixation by unicellular diazotrophs in the oligotrophic Pacific Ocean. *Nature*, *430*(7003), 1027–1031. https://doi.org/10.1038/nature02824

Moore, L. R., & Chisholm, S. W. (1999). Photophysiology of the marine cyanobacterium *Prochlorococcus*: Ecotypic differences among cultured isolates. *Limnology and Oceanography*, *44*(3), 628–638. https://doi.org/10.4319/lo.1999.44.3.0628

Moore, L. R., Rocap, G., & Chisholm, S. W. (1998). Physiology and molecular phylogeny of coexisting *Prochlorococcus* ecotypes. *Nature*, *393*(6684), Article 6684. https://doi.org/10.1038/30965

Moore, W. S. (1984). Review of the GEOSECS project. *Nuclear Instruments and Methods in Physics Research*, *223*(2–3), 459–465. https://doi.org/10.1016/0167-5087(84)90692-6

Moreno, A. R., & Martiny, A. C. (2018). Ecological stoichiometry of ocean plankton. *Annual Review of Marine Science*, *10*(1), 43–69. https://doi.org/10.1146/annurev-marine-121916-063126

Noh, K. M., Lim, H.-G., & Kug, J.-S. (2022). Global chlorophyll responses to marine heatwaves in satellite ocean color. *Environmental Research Letters*, *17*(6), 064034. https://doi.org/10.1088/1748-9326/ac70ec

Olson, R. J., Chisholm, S. W., Zettler, E. R., & Armbrust, E. V. (1990). Pigments, size, and distributions of *Synechococcus* in the north Atlantic and Pacific oceans. *Limnology and Oceanography*, *35*(1), 45–58. https://doi.org/10.4319/lo.1990.35.1.0045

Partensky, F., Blanchot, J., & Vaulot, D. (1999). Differential distribution and ecology of *Prochlorococcus* and *Synechococcus* in oceanic waters: A review. *Bulletin-Institut Oceanographique Monaco-Numero Special-*, 457–476.

Partensky, F., & Garczarek, L. (2010). *Prochlorococcus*: advantages and limits of minimalism. *Annual Review of Marine Science*, *2*(1), 305–331. https://doi.org/10.1146/annurev-marine-120308-081034

Partensky, F., Hess, W., & Vaulot, D. (1999). *Prochlorococcus*, a marine photosynthetic prokaryote of global significance. *Microbiology and Molecular Biology Reviews : MMBR*, *63*, 106–127. https://doi.org/10.1128/MMBR.63.1.106-127.1999

Petrou, K., Kranz, S. A., Trimborn, S., Hassler, C. S., Ameijeiras, S. B., Sackett, O., Ralph, P. J., & Davidson, A. T. (2016). Southern Ocean phytoplankton physiology in a changing climate. *Journal of Plant Physiology*, *203*, 135–150. https://doi.org/10.1016/j.jplph.2016.05.004

Ratkowsky, D. A., Lowry, R. K., McMeekin, T. A., Stokes, A. N., & Chandler, R. E. (1983). Model for bacterial culture growth rate throughout the entire biokinetic temperature range. *Journal of Bacteriology*, *154*(3), 1222–1226. https://doi.org/10.1128/jb.154.3.1222-1226.1983

Ribalet, F., Swalwell, J., Clayton, S., Jiménez, V., Sudek, S., Lin, Y., Johnson, Z. I., Worden, A. Z., & Armbrust, E. V. (2015). Light-driven synchrony of *Prochlorococcus* growth and mortality in the subtropical Pacific gyre. *Proceedings of the National Academy of Sciences*, *112*(26), 8008–8012. https://doi.org/10.1073/pnas.1424279112

Richardson, K., & Bendtsen, J. (2019). Vertical distribution of phytoplankton and primary production in relation to nutricline depth in the open ocean. *Marine Ecology Progress Series*, *620*, 33–46. https://doi.org/10.3354/meps12960

Rocap, G., Larimer, F. W., Lamerdin, J., Malfatti, S., Chain, P., Ahlgren, N. A., Arellano, A., Coleman, M., Hauser, L., Hess, W. R., Johnson, Z. I., Land, M., Lindell, D., Post, A. F., Regala, W., Shah, M., Shaw, S. L., Steglich, C., Sullivan, M. B., … Chisholm, S. W. (2003). Genome divergence in two *Prochlorococcus* ecotypes reflects oceanic niche differentiation. *Nature*, *424*(6952), Article 6952. https://doi.org/10.1038/nature01947

Rusch, D. B., Martiny, A. C., Dupont, C. L., Halpern, A. L., & Venter, J. C. (2010). Characterization of *Prochlorococcus* clades from iron-depleted oceanic regions.

Proceedings of the National Academy of Sciences, *107*(37), 16184–16189. https://doi.org/10.1073/pnas.1009513107

Siegel, D. A., Buesseler, K. O., Behrenfeld, M. J., Benitez-Nelson, C. R., Boss, E., Brzezinski, M. A., Burd, A., Carlson, C. A., D'Asaro, E. A., Doney, S. C., Perry, M. J., Stanley, R. H. R., & Steinberg, D. K. (2016). Prediction of the export and fate of global ocean net primary production: the EXPORTS science plan. *Frontiers in Marine Science*, *3*. https://www.frontiersin.org/articles/10.3389/fmars.2016.00022

Signorini, S. R., & McClain, C. R. (2012). Subtropical gyre variability as seen from satellites. *Remote Sensing Letters*, *3*(6), 471–479. https://doi.org/10.1080/01431161.2011.625053

Sloyan, B. M., Wanninkhof, R., Kramp, M., Johnson, G. C., Talley, L. D., Tanhua, T., McDonagh, E., Cusack, C., O'Rourke, E., McGovern, E., Katsumata, K., Diggs, S., Hummon, J., Ishii, M., Azetsu-Scott, K., Boss, E., Ansorge, I., Perez, F. F., Mercier, H., … Campos, E. (2019). The global ocean ship-based hydrographic investigations program (GO-SHIP): a platform for integrated multidisciplinary ocean science. *Frontiers in Marine Science*, *6*, 445. https://doi.org/10.3389/fmars.2019.00445

Smyth, T., Moffat, D., Tarran, G., Sathyendranath, S., Ribalet, F., & Casey, J. (2023). Determining drivers of phytoplankton carbon to chlorophyll ratio at Atlantic Basin scale. *Frontiers in Marine Science*, *10*, 1191216. https://doi.org/10.3389/fmars.2023.1191216

Sosik, H. M., Olson, R. J., Neubert, M. G., Shalapyonok, A., & Solow, A. R. (2003). Growth rates of coastal phytoplankton from time-series measurements with a submersible flow cytometer. *Limnology and Oceanography*, *48*(5), 1756–1765. https://doi.org/10.4319/lo.2003.48.5.1756

Staniewski, M. A., & Short, S. M. (2018). Methodological review and meta-analysis of dilution assays for estimates of virus- and grazer-mediated phytoplankton mortality. *Limnology and Oceanography: Methods*, *16*(10), 649–668. https://doi.org/10.1002/lom3.10273

Stewart, R. H. (2008). *Introduction to Physical Oceanography*. Texas A and M. https://oaktrust.library.tamu.edu/handle/1969.1/160216

Talley, L. D., Feely, R. A., Sloyan, B. M., Wanninkhof, R., Baringer, M. O., Bullister, J. L., Carlson, C. A., Doney, S. C., Fine, R. A., Firing, E., Gruber, N., Hansell, D. A., Ishii, M., Johnson, G. C., Katsumata, K., Key, R. M., Kramp, M., Langdon, C., Macdonald, A. M., … Zhang, J.-Z. (2016). Changes in ocean heat, carbon content, and ventilation: a review of the first decade of GO-SHIP global repeat hydrography. *Annual Review of Marine Science*, *8*(1), 185–215. https://doi.org/10.1146/annurev-marine-052915-100829

Tanioka, T., Larkin, A. A., Moreno, A. R., Brock, M. L., Fagan, A. J., Garcia, C. A., Garcia, N. S., Gerace, S. D., Lee, J. A., Lomas, M. W., & Martiny, A. C. (2022). Global ocean particulate organic phosphorus, carbon, oxygen for respiration, and nitrogen (GO-POPCORN). *Scientific Data*, *9*(1), 688. https://doi.org/10.1038/s41597-022-01809-1

Tarran, G. A., Heywood, J. L., & Zubkov, M. V. (2006). Latitudinal changes in the standing stocks of nano- and picoeukaryotic phytoplankton in the Atlantic Ocean. *Deep Sea Research Part II: Topical Studies in Oceanography*, *53*(14–16), 1516–1529. https://doi.org/10.1016/j.dsr2.2006.05.004

Taucher, J., & Oschlies, A. (2011). Can we predict the direction of marine primary production change under global warming? *Geophysical Research Letters*, *38*(2). https://doi.org/10.1029/2010GL045934

Thomas, M. K., Aranguren-Gassis, M., Kremer, C. T., Gould, M. R., Anderson, K., Klausmeier, C. A., & Litchman, E. (2017). Temperature–nutrient interactions exacerbate sensitivity to warming in phytoplankton. *Global Change Biology*, *23*(8), 3269–3280. https://doi.org/10.1111/gcb.13641

Ustick, L. J., Larkin, A. A., Garcia, C. A., Garcia, N. S., Brock, M. L., Lee, J. A., Wiseman, N. A., Moore, J. K., & Martiny, A. C. (2021). Metagenomic analysis reveals global-scale patterns of ocean nutrient limitation. *Science*, *372*(6539), 287–291. https://doi.org/10.1126/science.abe6301

Ustick, L. J., Larkin, A. A., & Martiny, A. C. (2023). Global scale phylogeography of functional traits and microdiversity in *Prochlorococcus*. *The ISME Journal*, *17*(10), 1671–1679. https://doi.org/10.1038/s41396-023-01469-y

Vaulot, D., & Marie, D. (1999). Diel variability of photosynthetic picoplankton in the equatorial Pacific. *Journal of Geophysical Research: Oceans*, *104*(C2), 3297–3310. https://doi.org/10.1029/98JC01333

Wilson, C. (2011). Chlorophyll anomalies along the critical latitude at 30°N in the NE Pacific. *Geophysical Research Letters*, *38*(15), 2011GL048210. https://doi.org/10.1029/2011GL048210

Wilson, C., & Qiu, X. (2008). Global distribution of summer chlorophyll blooms in the oligotrophic gyres. *Progress in Oceanography*, *78*(2), 107–134. https://doi.org/10.1016/j.pocean.2008.05.002

Wilson, C., Villareal, T. A., Brzezinski, M. A., Krause, J. W., & Shcherbina, A. Y. (2013). Chlorophyll bloom development and the subtropical front in the North Pacific. *Journal of Geophysical Research: Oceans*, *118*(3), 1473–1488. https://doi.org/10.1002/jgrc.20143

Woods, J. D. (1985). The World Ocean Circulation Experiment. *Nature*, *314*(6011), 501–511. https://doi.org/10.1038/314501a0

Worden, A. Z., & Binder, B. J. (2003). Application of dilution experiments for measuring growth and mortality rates among *Prochlorococcus* and *Synechococcus* populations in oligotrophic environments. *Aquatic Microbial Ecology*, *30*(2), 159–174. https://doi.org/10.3354/ame030159

Wu, L., Cai, W., Zhang, L., Nakamura, H., Timmermann, A., Joyce, T., McPhaden, M. J., Alexander, M., Qiu, B., Visbeck, M., Chang, P., & Giese, B. (2012). Enhanced warming over the global subtropical western boundary currents. *Nature Climate Change*, *2*(3), 161–166. https://doi.org/10.1038/nclimate1353

Zinser, E. R., Johnson, Z. I., Coe, A., Karaca, E., Veneziano, D., & Chisholm, S. W. (2007). Influence of light and temperature on *Prochlorococcus* ecotype distributions in the Atlantic Ocean. *Limnology and Oceanography*, *52*(5), 2205–2220. https://doi.org/10.4319/lo.2007.52.5.2205

Appendices

Appendix 1: Side Scatter to Carbon Conversion

CULTURE	Phytoplankton Group	ug C/ml	stdev	CV	#/ml	nFSC	pg C/cell	CYTEK FSC Geo mean	CYTEK SSC Geo mean
MED4	*Prochlorococcus*	3.24817778	0.012381	0.00381168	951407.186	0.02	0.03414077	1386	7736
7803	*Synechococcus*	11.7985222	0.38532904	0.03265909	210354.687	0.265	0.56088706	22238	86420
WH8102	*Synechococcus*	11.5517667	0.22956946	0.0198731	441825.722	0.21	0.26145528	12773	32928
AS9601	*Prochlorococcus*	8.92685556	0.43586755	0.04882655	1740483.57	0.04	0.05128951	1948	10368
1314	*Prochlorococcus*	0.7182	0.07663064	0.10669818	189337.465	0.03	0.03793227	1417	10516
NAT12A	*Prochlorococcus*	0.38396667	0.05817511	0.15151083	43857.1565	0.06	0.08754938	2063	13193

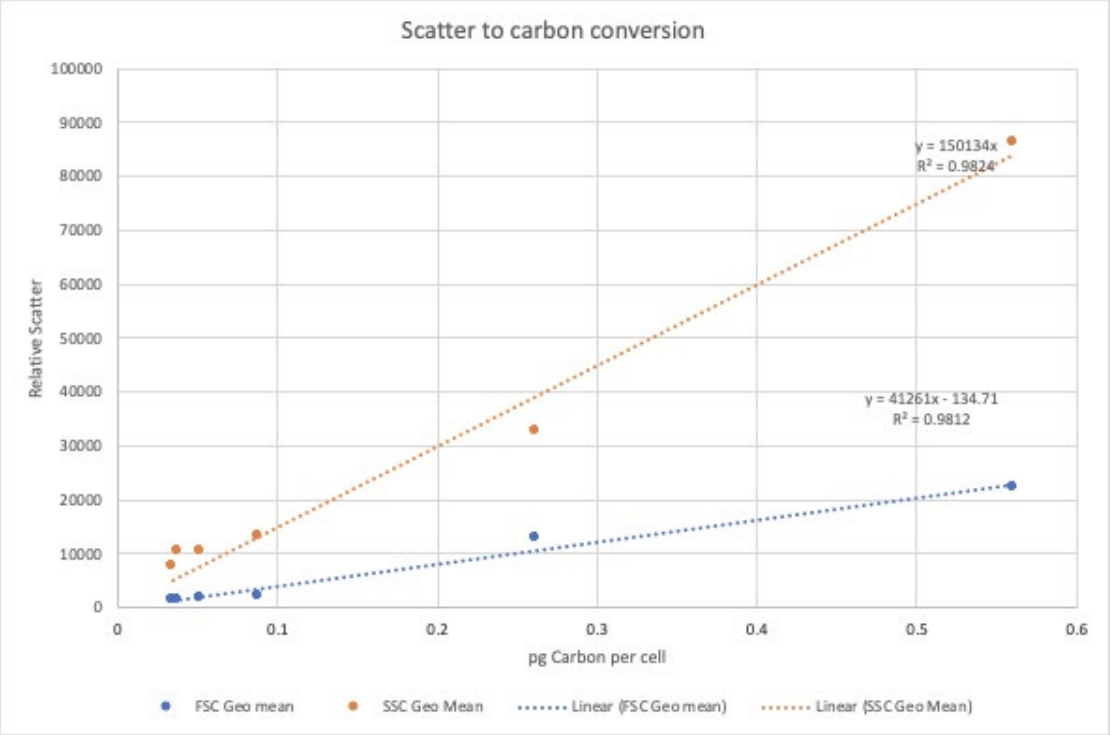

Appendix 1. Linear relationship for forward scatter and side scatter data, processed by the Cytek Northern Lights Flow Cytometer, to convert geometric mean side scatter (SSC) and forward scatter (FSC) data to picograms of carbon per cell. Conversion factors (CV) were determined based on five different plankton cultures. Data courtesy of Nicole Poulton of the Center for Aquatic Cytometry at the Bigelow Laboratory for Ocean Sciences.